



A National Center of Excellence in Advanced Technology Applications

ISSN 1520-295X

Hysteretic Models for Cyclic Behavior of Deteriorating Inelastic Structures

by

M.V. Sivaselvan and A.M. Reinhorn

University at Buffalo, State University of New York
Department of Civil, Structural and Environmental Engineering
Ketter Hall
Buffalo, New York 14260

Technical Report MCEER-99-0018

November 5, 1999

This research was conducted at the University of Buffalo, State University of New York and was supported in whole or in part by the National Science Foundation under Grant No. CMS 97-01471 and other sponsors.

NOTICE

This report was prepared by the University at Buffalo, State University of New York as a result of research sponsored by the Multidisciplinary Center for Earthquake Engineering Research (MCEER) through a grant from the National Science Foundation and other sponsors. Neither MCEER, associates of MCEER, its sponsors, the University at Buffalo, State University of New York, nor any person acting on their behalf:

- a. makes any warranty, express or implied, with respect to the use of any information, apparatus, method, or process disclosed in this report or that such use may not infringe upon privately owned rights; or
- b. assumes any liabilities of whatsoever kind with respect to the use of, or the damage resulting from the use of, any information, apparatus, method, or process disclosed in this report.

Any opinions, findings, and conclusions or recommendations expressed in this publication are those of the author(s) and do not necessarily reflect the views of MCEER, the National Science Foundation, or other sponsors.

Hysteretic Models for Cyclic Behavior of Deteriorating Inelastic Structures

by

M.V. Sivaselvan¹ and A.M. Reinhorn²

Publication Date: November 5, 1999

Submittal Date: April 22, 1999

Technical Report MCEER-99-0018

Task Numbers 99-1502, 99-4101, 98-1502 and 98-1451

NSF Master Contract Number CMS 97-01471

- 1 Ph.D. Candidate, Department of Civil, Structural and Environmental Engineering, University at Buffalo, State University of New York
- 2 Professor, Department of Civil, Structural and Environmental Engineering, University at Buffalo, State University of New York

MULTIDISCIPLINARY CENTER FOR EARTHQUAKE ENGINEERING RESEARCH
University at Buffalo, State University of New York
Red Jacket Quadrangle, Buffalo, NY 14261

Preface

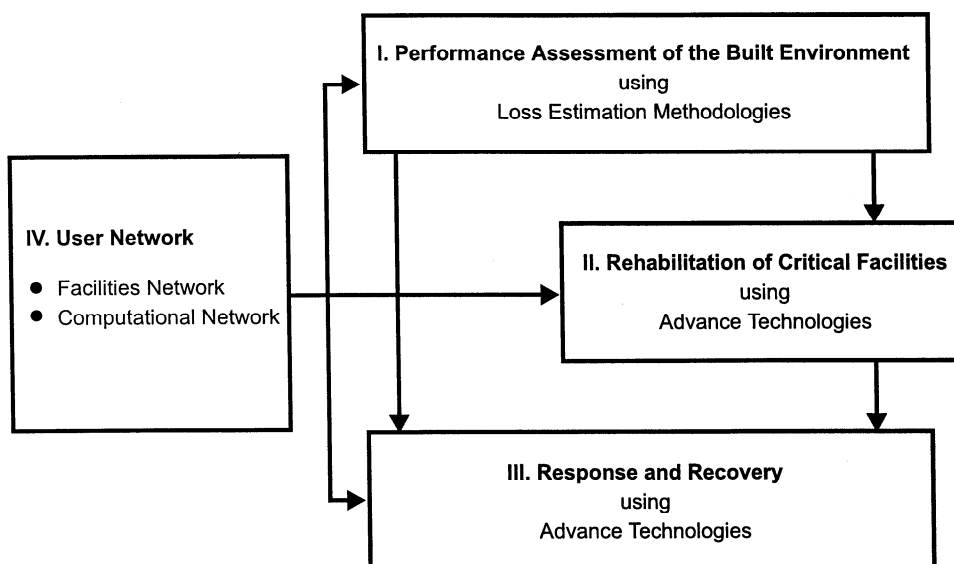
The Multidisciplinary Center for Earthquake Engineering Research (MCEER) is a national center of excellence in advanced technology applications that is dedicated to the reduction of earthquake losses nationwide. Headquartered at the University at Buffalo, State University of New York, the Center was originally established by the National Science Foundation in 1986, as the National Center for Earthquake Engineering Research (NCEER).

Comprising a consortium of researchers from numerous disciplines and institutions throughout the United States, the Center's mission is to reduce earthquake losses through research and the application of advanced technologies that improve engineering, pre-earthquake planning and post-earthquake recovery strategies. Toward this end, the Center coordinates a nationwide program of multidisciplinary team research, education and outreach activities.

MCEER's research is conducted under the sponsorship of two major federal agencies: the National Science Foundation (NSF) and the Federal Highway Administration (FHWA), and the State of New York. Significant support is derived from the Federal Emergency Management Agency (FEMA), other state governments, academic institutions, foreign governments and private industry.

The Center's NSF-sponsored research is focused around four major thrusts, as shown in the figure below:

- quantifying building and lifeline performance in future earthquake through the estimation of expected losses;
- developing cost-effective, performance based, rehabilitation technologies for critical facilities;
- improving response and recovery through strategic planning and crisis management;
- establishing two user networks, one in experimental facilities and computing environments and the other in computational and analytical resources.



For several years now, MCEER has supported research associated with developing nonlinear time history modeling strategies for structural systems. An important element of these codes is for the user to have an appreciation of the strengths and weaknesses, pitfalls, advantages and disadvantages of the various types of hysteretic models employed. In the past, users of various nonlinear time history analysis programs have needed to be very adept in assigning values for the various parameters that control hysteretic rules, as little documentation was available. More recently, there has been an increased awareness and the use of nonlinear time history analysis programs in professional engineering practice. Instead of developing better programs, there is a need to operate existing programs in a smarter fashion. Therefore, the purpose of this report is: (1) to provide a theoretical basis for a range of rule-based piecewise linear hysteretic models (in Section 2), as well as differential equation-based smooth hysteric models (in Section 3); and (2) to provide a sound and formal reasoning for the basis of the above-mentioned models that are founded on the fundamentals of mechanics and the interrelationship between these various types of models (in Section 4). This research fits in with two of MCEER's missions: outreach to the professional user community; and to extend the fundamental knowledge base to enable a high level of computational simulation to be conducted.

ABSTRACT

Two versatile hysteretic models for inelastic behavior of macro-models of structural components— a polygonal model and a smooth model - have been developed. These models have the capability of simulating deteriorating behavior of strength, stiffness and bond slip. The theoretical background, the development and the implementation of these models are presented. The report attempts to show a holistic picture of the modeling of one-dimensional inelastic material behavior and indicates how various hysteretic models fit into this framework. It is shown that the models developed herein are obtained from the basic principles of mechanics and thermodynamics through numerous assumptions, which lead to certain approximations. Finally, the incorporation of the hysteretic models into two computer platforms for nonlinear analysis – IDARC2D and NSPECTRA – is described.

ACKNOWLEDGEMENTS

This research was carried out by the authors at the Department of Civil, Structural and Environmental Engineering, University at Buffalo. Financial support from the Multidisciplinary Center for Earthquake Engineering Research (Project Nos.: 991502, 994101, 981502 and 981451, supported in turn by NSF and 106E.7.2.3 and 106E.7.5, supported in turn by FHWA) is gratefully acknowledged.

TABLE OF CONTENTS

SECTION	TITLE	PAGE
1	INTRODUCTION	1
2	THE POLYGONAL HYSTERETIC MODEL (PHM)	5
2.1	Backbone Curves and Types of Cyclic Behavior	6
2.2	“Points” and “Branches”	6
2.3	Operation of the Model – Force Vs. Displacement Control (Moment/Curvature Controlled)	7
2.4	Degradation	9
2.4.1	Stiffness Degradation	9
2.4.2	Strength Degradation	11
2.4.3	Pinching or Slip	14
2.5	Algorithm and Implementation	14
2.6	Examples	19
3	THE SMOOTH HYSTERETIC MODEL (SHM)	21
3.1	Plain Hysteretic Behavior without Degradation	21
3.1.1	Spring 1: Post-yield Spring	21
3.1.2	Spring 2: Hysteretic Spring	23
3.2	Degradation	24
3.2.1	Stiffness Degradation	24
3.2.2	Strength Degradation	24
3.2.3	Pinching or Slip	25
3.3	Gap Closing Behavior	28
3.4	Solution of the SHM	28
3.5	Examples	33
4	UNIFICATION OF CONCEPTS FOR REPRESENTATION OF INELASTIC MATERIAL BEHAVIOR IN ONE DIMENSION	39
4.1	Background	39
4.2	Algebraic Models	43
4.2.1	Masing’s Hypothesis (Beck and Jayakumar, 1996)	43
4.2.2	Ramberg-Osgood Model	43
4.3	Differential Equation Models	44
4.3.1	Plasticity Based on Yield Surface	44
4.3.2	Plasticity/Viscoplasticity without a Yield Surface	45
4.3.3	Endochronic Theory	46
4.3.4	Ozdemir Model (Ozdemir, 1976)	47
4.3.5	Wen-Bouc Model	51

TABLE OF CONTENTS (cont'd)

SECTION	TITLE	PAGE
4.3.6	Spring and Slider models	54
4.3.7	Integral formulation of Spring and Slider Models	55
4.3.8	Smooth Plasticity Models and Drucker's Stability Postulate	58
4.4	Other Strength Degradation Rules	59
5	IMPLEMENTATION IN COMPUTER PROGRAMS	63
5.1	Background	63
5.2	IDARC2D Version 5.0	63
5.2.1	Implementation of Hysteretic Model	64
5.2.2	Example	64
5.3	NSPECTRA	68
5.3.1	Implementation of Hysteretic Model	68
5.3.2	Examples	68
6	CONCLUSIONS AND REMARKS	71
7	REFERENCES	73
Appendix A	IMPLEMENTATION DETAILS OF THE POLYGONAL HYSTERETIC MODEL	A-1

LIST OF ILLUSTRATIONS

FIGURE	TITLE	PAGE
2.1	Backbone Curves	8
2.2	Types of Cyclic Behavior	8
2.3	Illustration of Branch Transition	8
2.4	Points and Branches of the PHM	10
2.5	Modeling of Stiffness Degradation for Positive Excursion	12
2.6	Schematic Representation of Strength Degradation in the PHM	13
2.7	Modeling of Slip	13
2.8	Overall Flow of PHM Module	15
2.9	Flowchart for Subroutine CONTROL1	16
2.10	Flowchart for Subroutine CONTROL2	17
2.11	Flowchart for Subroutine CONTROL3	18
2.12	Examples of Hysteretic Behavior Modeled by the PHM	20
3.1	Two-Spring Model for Non-Degrading Hysteretic Behavior	22
3.2	Three-Spring Model for Hysteretic Behavior with Slip	27
3.3	Gap-Closing Spring in Parallel	29
3.4	Examples of Hysteretic Behavior Modeled by the SHM	34
4.1	Spring and Dashpot Representation of Linear Viscoelastic Material	41
4.2	Development of Ozdemir's Model	48
4.3	Spring and Slider Model	56
4.4	Integral Formulation of Spring and Slider Models	56
4.5	Smooth Model and Drucker's Postulate	60
4.6	Schematic Diagram of Representation of 1D Inelastic Behavior	61
5.1	The Method of One-Step Correction	65
5.2	Configuration and Loading of Test Structure for IDARC Example	66
5.3	Force-Displacement Response of IDARC Example	67
5.4	Example from NSPECTRA	69
A.1	Explanation for Rules which change Branches from 2 to 21 and 3 to 20	A-21

LIST OF TABLES

TABLE	TITLE	PAGE
3.1	Range of Parameters	35
3.2	Results from Connection Tests (SAC Joint Venture, 1996)	36
A.1	Subroutines and their functions	A-1
A.2	Variables Governing PHM	A-2
A.3	Point Formulas	A-4
A.4	Map of Branch Connectivity	A-10
A.5	Starting and ending points of branches	A-13
A.6	Rules for Change of Branch	A-14

SECTION 1

INTRODUCTION

Hysteresis is a highly nonlinear phenomenon occurring in many fields involving systems that possess memory, including inelasticity, electricity, magnetism etc. Structures when subjected to dynamic loading under strong earthquake excitation usually exhibit hysteretic behavior. Different structural members and connections are deliberately designed and detailed to dissipate energy by hysteresis to increase the margin of safety against seismic collapse (Mazzolani and Piluso, 1996, Priestley and Calvi, 1996, Bruneau et al, 1998). Often, special energy dissipating devices are introduced into structural systems for this purpose (Casper and Reinhorn, 1986, Soong and Dargush, 1997). The dissipation of energy may be due to inelastic material behavior, interface friction, etc. However, under repeated cyclic deformation, there is invariably deterioration in the characteristics of such hysteretic loops. Such deterioration must be taken into account in the modeling and design of seismic-resistant structural systems.

The structural engineering community is moving towards fragility analysis and performance-based approaches for more rational seismic-resistant structural design. The underlying assumption of such methods is that the level of damage suffered by a structure due to a given seismic event can be quantitatively predicted. Therefore, more knowledge about structural behavior beyond the onset of damage is needed to bring such methods to maturity. Analyses must be conducted to correlate and quantify the stages of damage with respect to the level of ground shaking and to evaluate the effectiveness of innovative structural devices and retrofit measures. The basic requirement of such analyses is the

availability of accurate constitutive models capable of representing deteriorating structural behavior and their implementation in computer programs to perform nonlinear structural analysis.

Several such hysteretic models have been developed. These can be broadly classified into two types – Polygonal Hysteretic Models (PHM) and Smooth Hysteretic Models (SHM). Examples of the first kind are Clough's model (Clough, 1966), Takeda's model (Takeda et al, 1970) and the Three-parameter Park model (Park et al, 1987). The Wen-Bouc model (Bouc, 1967 and Wen, 1976) and Ozdemir's model (Ozdemir, 1976), on the other hand are examples of the latter kind. Thyagarajan (1989) discusses a discrete element model (DEM) for hysteretic behavior based on the concept proposed by Iwan (1966). This is a polygonal model that becomes smooth in the limit of infinite elements. Many of these models that are in popular use have been developed independent of each other based on different behavioral, physical or mathematical motivations. However, closer examination would show that they share several features and stem from a common theoretical base. One of the aspects of this work is to establish this common basis. Such an understanding is important in developing new models and in recognizing physical limitations of many existing models.

The objectives of the work reported here are:

- (a) To develop two versatile hysteretic models – PHM and SHM – with stiffness and strength deterioration and pinching characteristics.

- (b) To present a holistic picture of the modeling of one-dimensional inelastic material behavior and justify the use of such models to represent the relationships between stress-resultants and strains.
- (c) To discuss various numerical solution schemes for nonlinear problems involving the hysteretic models developed and to demonstrate the implementation of the models in two computational platforms – IDARC2D and NSPECTRA.

The development of the Polygonal Hysteretic Model is presented in Section 2. Section 3 discusses the Smooth Hysteretic Model. The theoretical concerns of objective (b) are explained in Section 4. The implementation of the two hysteretic models in computer platforms is shown in Section 5. Section 6 summarizes the work reported and presents some important conclusions.

The hysteretic models presented here were developed in the context of moment-curvature relationships of beam-columns. Therefore Sections 2 and 3 refer to the stress variable as “Moment” (M) and the strain variable as “Curvature” (ϕ). However, these can be replaced by any other work-conjugate pair, according to the application under consideration.

SECTION 2

THE POLYGONAL HYSTERETIC MODEL (PHM)

Polygonal Hysteretic Models (PHM) refers to hysteretic models with piecewise linear behavior. They are also referred to as *multi-linear* models. The PHM may be embodied in the bilinear model, double bilinear model, origin-oriented model, peak-oriented model, slip model, etc. Such models are most often motivated by actual behavioral stages of an element or structure, such as, initial or elastic, cracking, yielding, stiffness and strength degrading stages, crack and gap closures, etc. The model parameters can represent and therefore can be explicitly assigned to actual physical quantities. These models are therefore governed by *rules* that fix distinct *points* and dictate the transitions between various stages or *branches* that occur during the response. It is however shown in Section 4, that such models conform to the general framework of inelastic material behavior and that under certain circumstances, they can be represented by a set of nonlinear differential equations involving internal variables.

Several PHM's have been developed, each to represent a specific type of behavior (Clough, 1966, Fukada, 1969, Takeda, 1970, Aoyama, 1971, Muto et al, 1973, Tani and Nomura, 1973, Atalay and Penzien, 1975, Kustu and Bouwkamp, 1975, Takayanagi, 1977, Nakata et al, 1978). Park et al (1987) present a comparative study of the features of these models. The PHM presented in this study is an extension of the Three-parameter Park Model (Park et al, 1987). A general framework of *points* and *branches* is developed which can represent any of the aforementioned PHM's as a special case and includes various forms of degradation. This framework along with the degradation rules is

discussed in the following paragraphs. The reformulation of the polygonal model was done such that the model is controlled by backbone curves specified by the material or structural properties. Furthermore, the cyclic behavior is represented by points and branches which are functions of the backbone parameters and the current instantaneous forces and deformations. The behavior along a branch and the changes of branches follow a logic tree.

2.1 Backbone Curves and Types of Cyclic Behavior

The PHM has been implemented with two types of backbone curves – Bilinear and Trilinear which accommodate cracking models in addition to yielding (Fig. 2.1). With trilinear backbone curve, the model can be used to establish two types of cyclic behavior – Yield-oriented with slip and Vertex-oriented (Fig. 2.2). In Fig. 2.4, points corresponding to bilinear behavior are denoted by primed numbers, and those of vertex-oriented behavior by double-primed numbers. The yield-oriented model with slip is the default and is denoted by unprimed points. The model is formulated in such a way that all of the above type of behavior has the same branch transition rules.

2.2 “Points” and “Branches”

The state of the entity, whose hysteresis is being modeled, is completely defined by a set of *database variables*. These database variables are listed Table A.2. It will be seen in Section 4 that these are nothing but *internal variables*. A number of *control points* on the hysteresis loop are completely defined by these database variables. If the values of these variables are known apriori, coordinates of the control points can be calculated using

functions shown in Table A.3. Lines between these points are called *branches* and represent the path along the hysteresis loop. Each branch leads to a set of other branches as shown in Table A.4. The end points of the branches are listed in Table A.5. The transitions between branches are governed by a set of rules (logic tree) as shown in Table A.6. The model discussed in this section uses 21 control points and 25 branches as shown in Fig. 2.4. Consider for example, unloading from branch 10, as shown in Fig. 2.3 (a). The rules of Table A.4 and Table A.6 that govern this transition are summarized in Fig. 2.3 (b) and (c).

2.3 Operation of the Model – Force Vs. Displacement Control (Moment/Curvature Controlled)

The PHM can be driven in three ways:

1. Force controlled – An incremental force is applied and the model responds by achieving that force increment and the corresponding displacement increment.
2. Quasi-force controlled – An incremental force is given; however, the corresponding displacement increment is calculated using the stiffness of the current branch. This displacement is applied to the model and it responds by achieving this displacement increment and returning the difference between the target force and the achieved force (capacity force). This method of driving the model is used while integrating by the method of one-step correction.
3. Displacement controlled – An incremental displacement is applied and the model responds by achieving that displacement increment and the corresponding force increment.

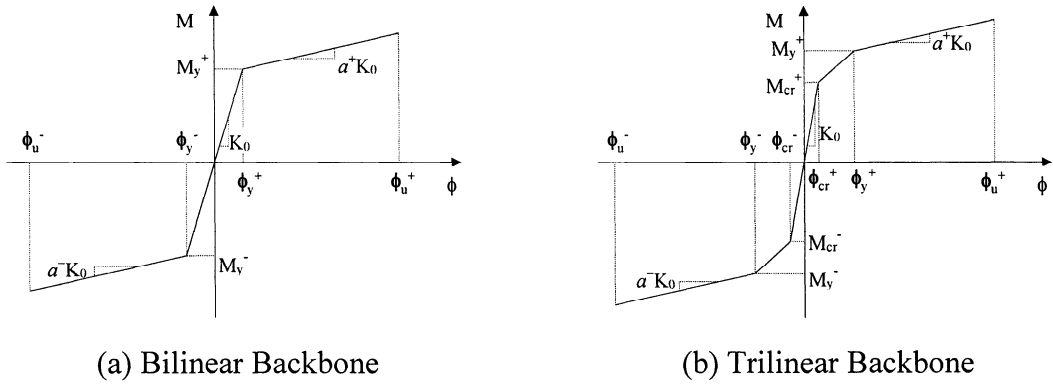


Fig. 2.1 Backbone Curves

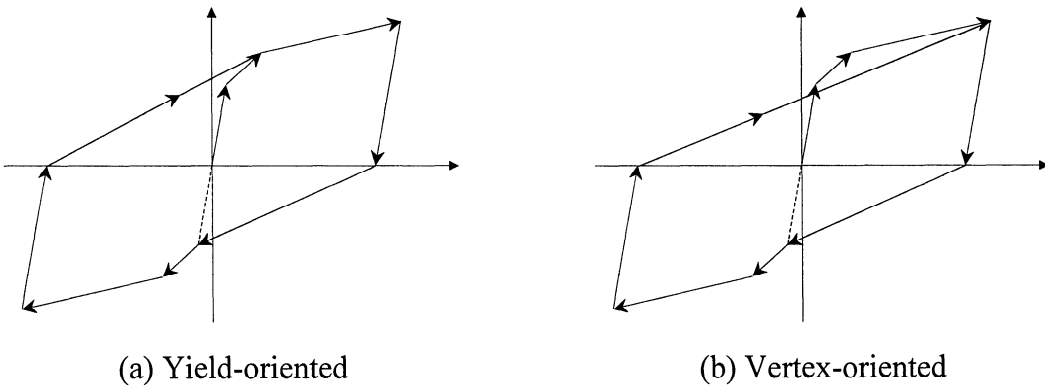


Fig. 2.2 Types of Cyclic Behavior

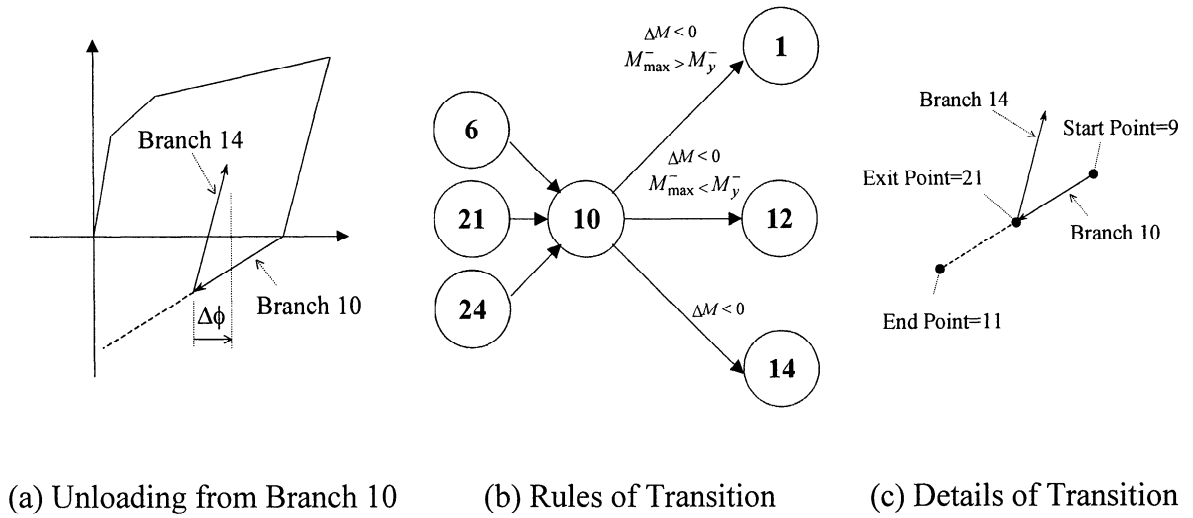


Fig. 2.3 Illustration of Branch Transition

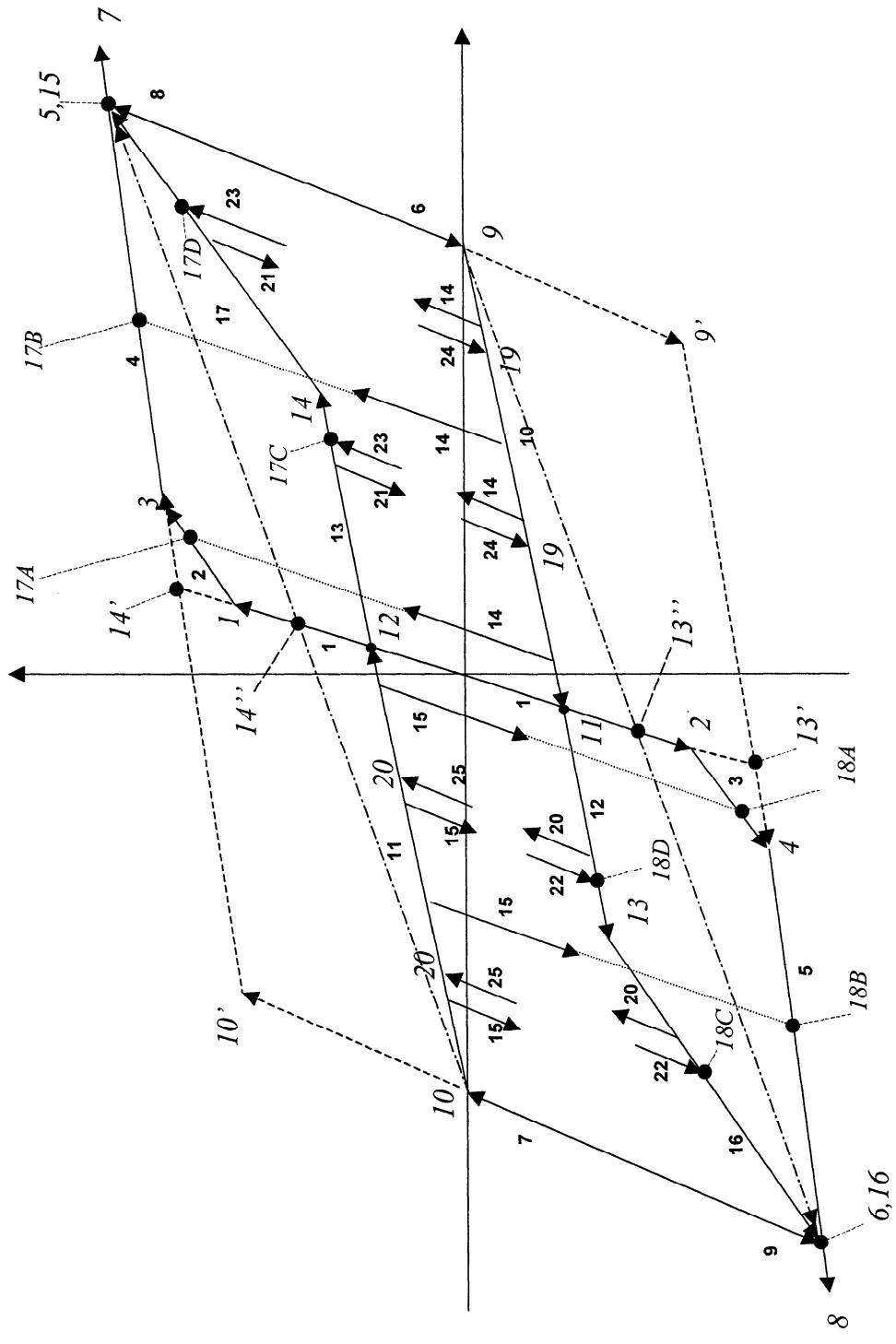


Fig. 2.4 Points and Branches of the PHM

2.4 Degradation

The modeling of stiffness and strength degradation, and pinching are discussed below.

2.4.1 Stiffness Degradation

Stiffness degradation occurs due to geometric effects. The elastic stiffness degrades with increasing ductility. It has been found that the phenomenon of stiffness degradation can be accurately modeled by the pivot rule (Park et al, 1987). According to this rule, the load-reversal branches are assumed to target a pivot point on the elastic branch at a distance of αM_y on the opposite side, where α is the stiffness degradation parameter. This is shown in Fig. 2.5. From the geometry in Fig. 2.5, it can be found that the stiffness degradation factor is given by,

$$R_K^+ = \frac{M_{cur} + \alpha M_y}{K_0 \phi_{cur} + \alpha M_y} \quad (2.1)$$

where M_{cur} = current moment, ϕ_{cur} = current curvature, K_0 = initial elastic stiffness, α = stiffness degradation parameter, $M_y = M_y^+$ if (M_{cur}, ϕ_{cur}) is on the right side of the elastic branch and $M_y = M_y^-$ if (M_{cur}, ϕ_{cur}) is on the left side of the elastic branch. The current elastic stiffness is given by,

$$K_{cur} = R_K K_0 \quad (2.2)$$

2.4.2 Strength Degradation

Strength degradation is modeled by reducing the capacity in the backbone curve as shown schematically in Fig. 2.6. It will be seen in Sections 3 and 4, that this is equivalent to specifying an evolution equation for the yield moment. The strength degradation rule is given by,

$$M_y^{+/-} = M_{y0}^{+/-} \left[1 - \left(\frac{\phi_{\max}^{+/-}}{\phi_u^{+/-}} \right)^{\frac{1}{\beta_1}} \right] \left[1 - \frac{\beta_2}{1 - \beta_2} \frac{H}{H_{ult}} \right] \quad (2.3)$$

where $M_y^{+/-}$ = positive or negative yield moment, $M_{y0}^{+/-}$ = initial positive or negative yield moment, $\phi_{\max}^{+/-}$ = maximum positive or negative curvature, $\phi_u^{+/-}$ = positive or negative ultimate curvature, h = hysteretic energy dissipated, h_{ult} = hysteretic energy dissipated when loaded monotonically to the ultimate curvature without any degradation, β_1 = ductility-based strength degradation parameter and β_2 = energy-based strength degradation parameter.

The second term on the right-hand side of equation (2.3) represents strength degradation due to increased deformation and the third term represents strength degradation due to hysteretic energy dissipated. The increment of the hysteretic energy is given by,

$$\Delta H = \left[\frac{M + (M + \Delta M)}{2} \right] \left(\Delta \phi - \frac{\Delta M}{R_K K_0} \right) \quad (2.4)$$

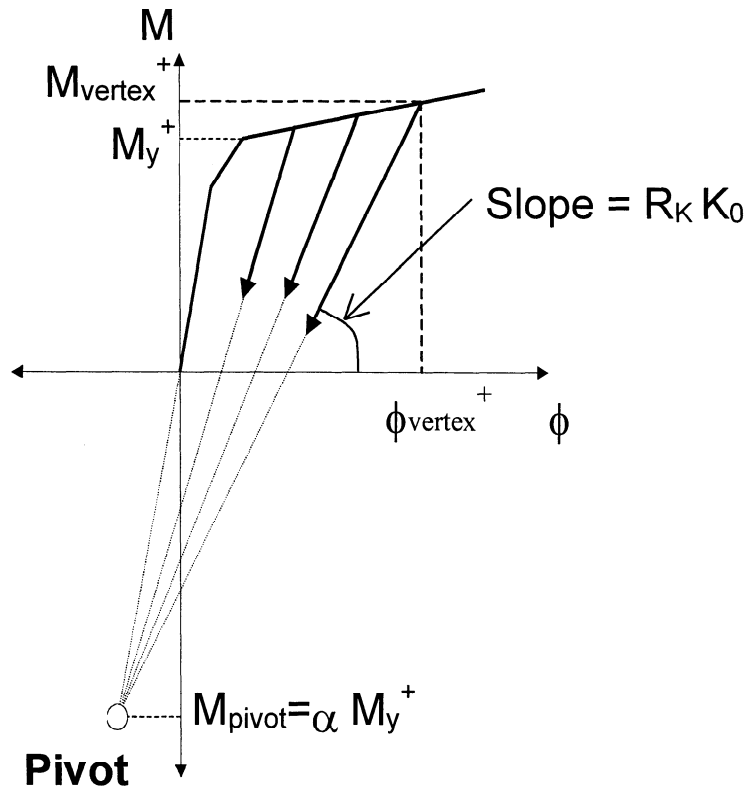


Fig. 2.5 Modeling of Stiffness Degradation for Positive Excursion.

(for negative excursion the “+” sign changes accordingly)

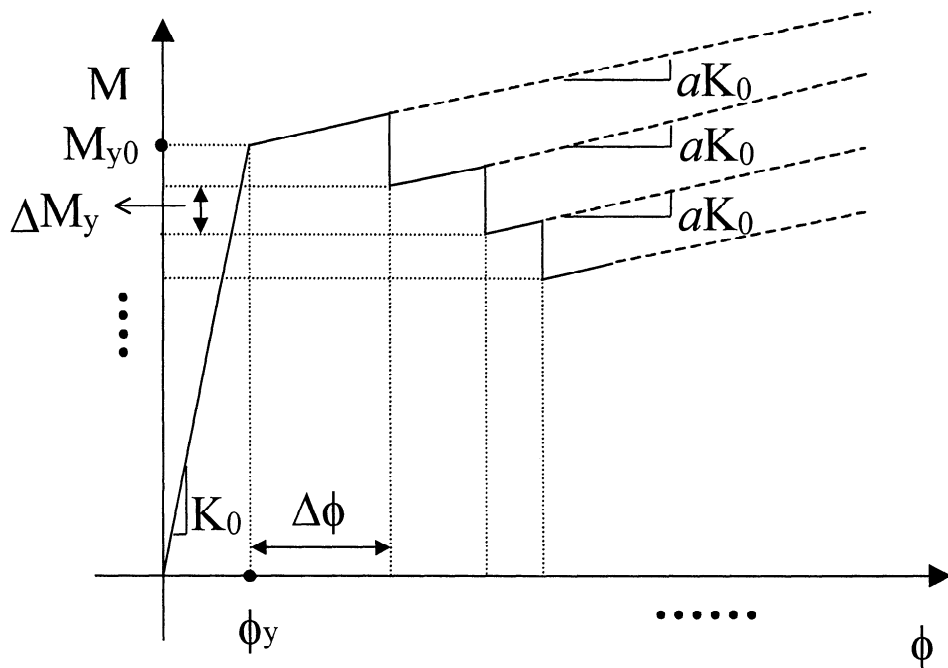


Fig. 2.6 Schematic Representation of Strength Degradation in the PHM

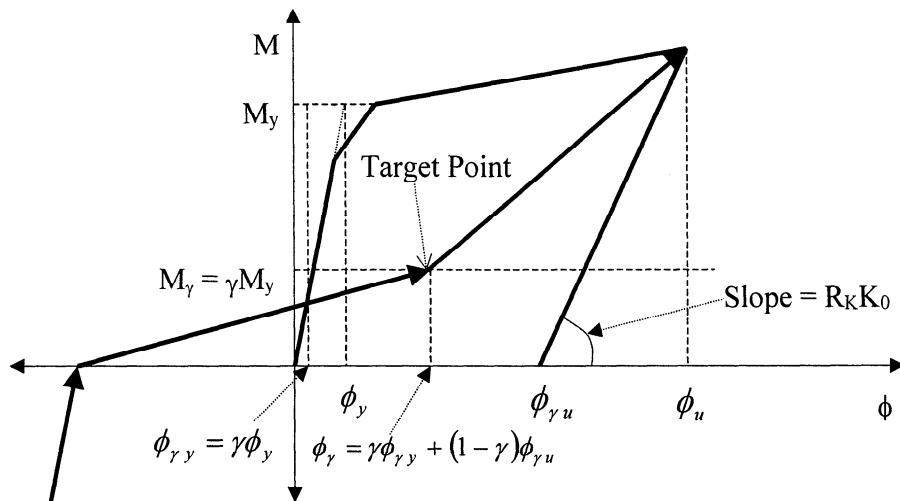


Fig. 2.7 Modeling of Slip

2.4.3 Pinching or Slip

Slip or pinching occurs as a result of crack closure, bolt slip, etc. Slip is modeled by defining the target point for the loading branch to be the crack closing point. The force level corresponding to this point is a fraction of the yield moment given by $F\gamma = \gamma F_y$, and the deformation level is obtained as a weighted average of the yield and ultimate deformations as shown in Fig. 2.7. γ is the slip parameter.

2.5 Algorithm and Implementation

The PHM is implemented using a number of subroutines. These subroutines and their functions are listed in Table A.1. The algorithms of these subroutines are shown in Fig. 2.8 - Fig. 2.11

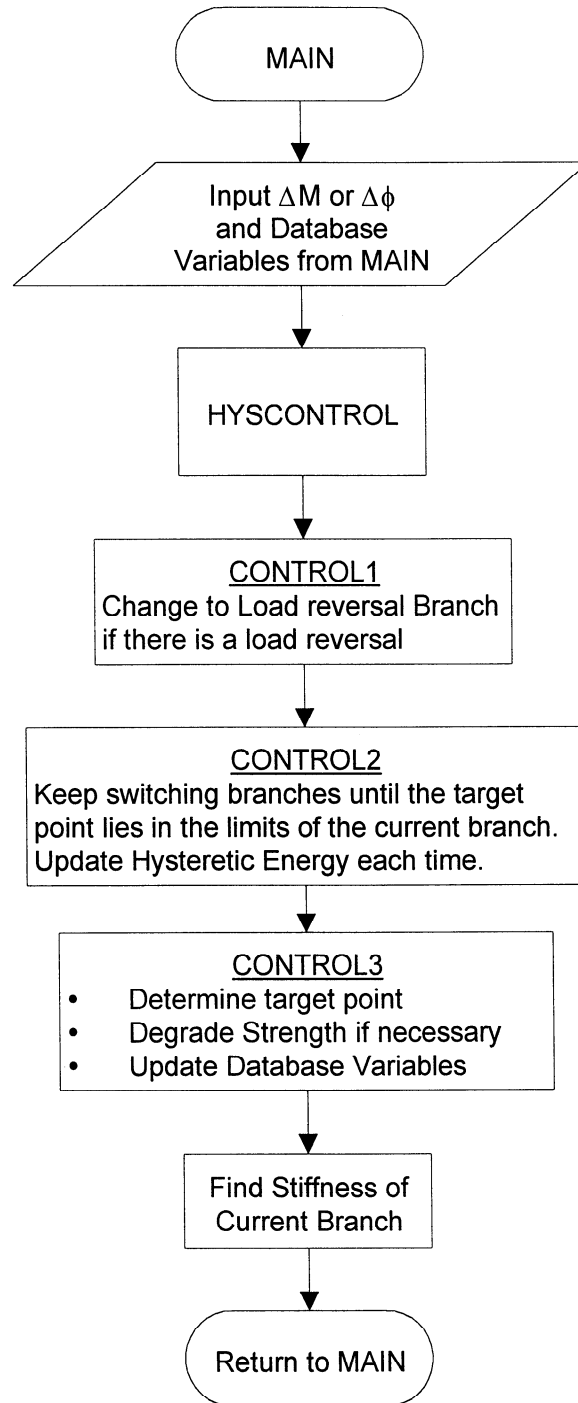


Fig. 2.8 Overall Flow of PHM Module

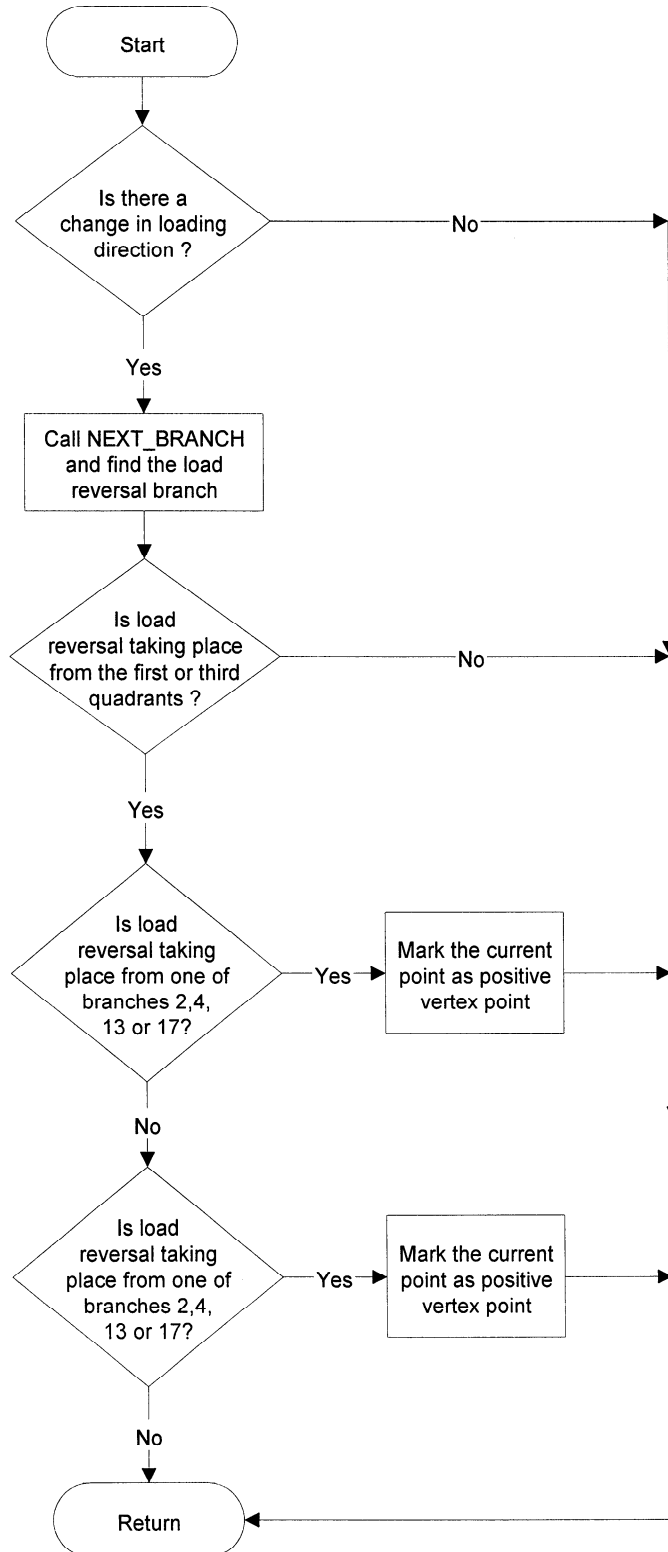


Fig. 2.9 Flowchart for Subroutine CONTROL1

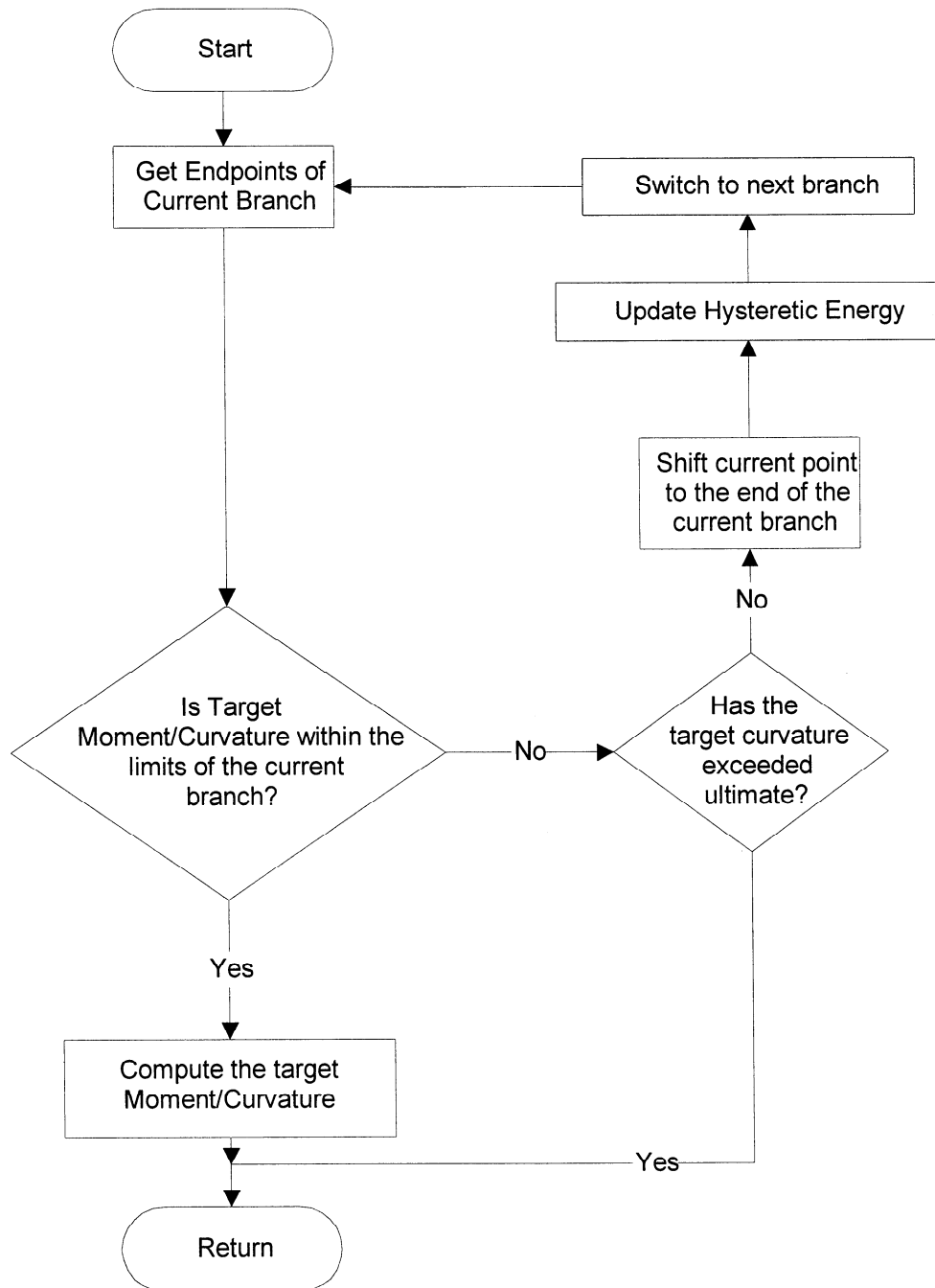


Fig. 2.10 Flowchart for Subroutine CONTROL2

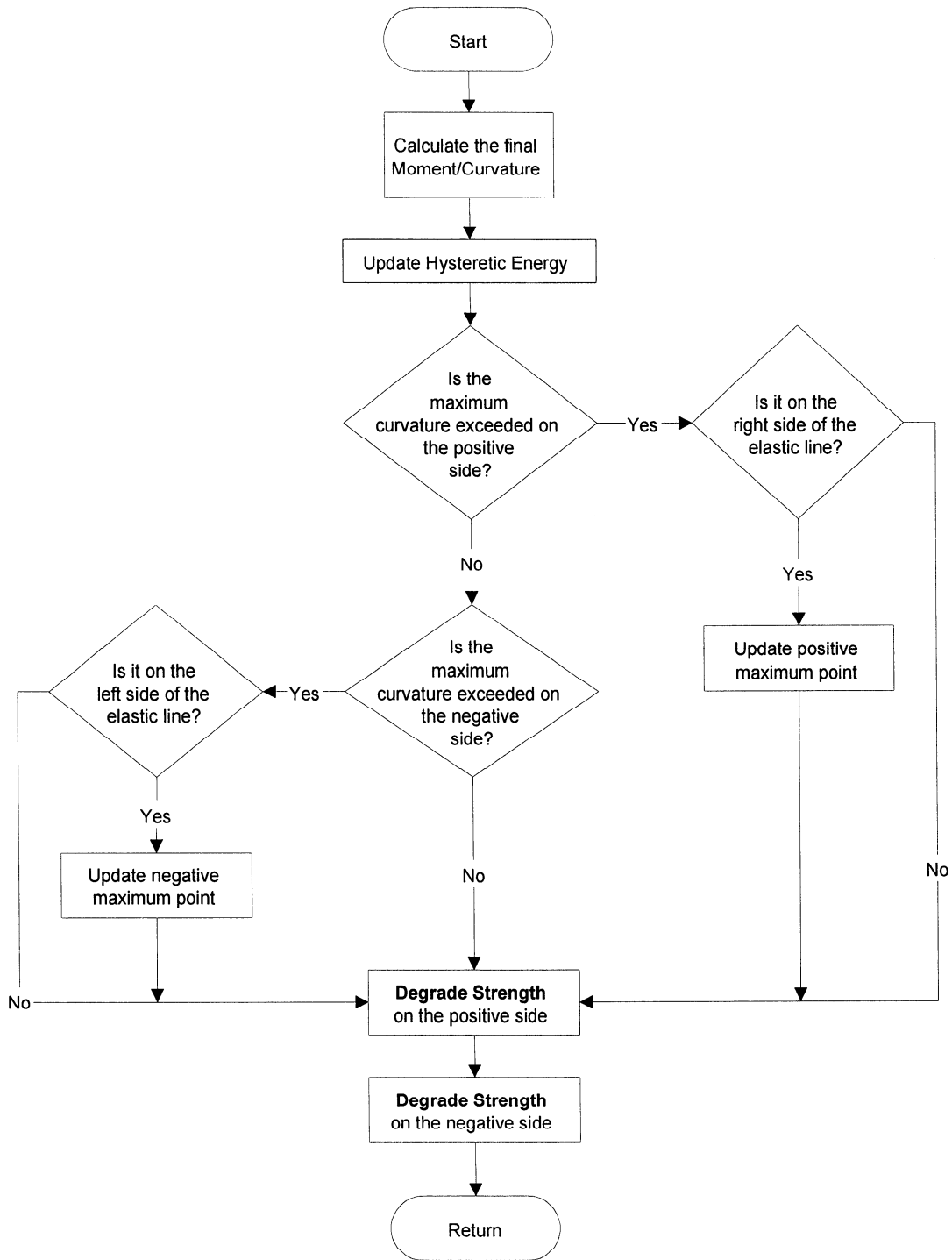
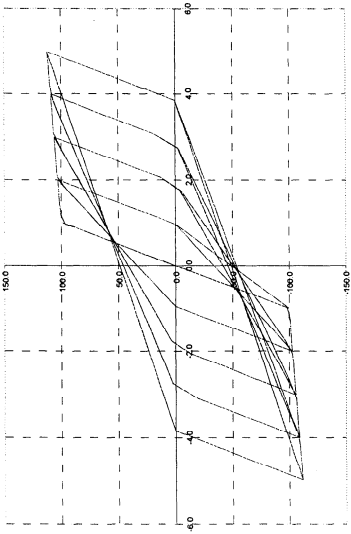


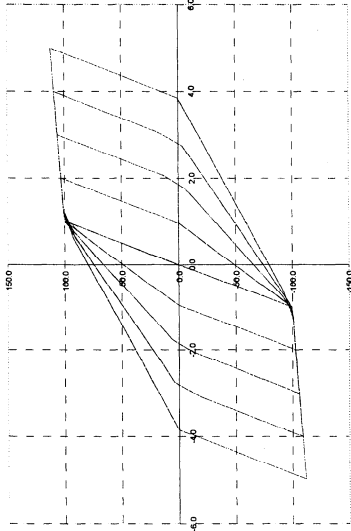
Fig. 2.11 Flowchart for Subroutine CONTROL3

2.6 Examples

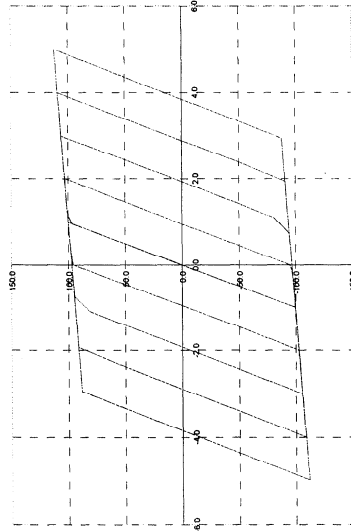
Examples of various types of hysteretic behavior modeled by the PHM are shown in Fig. 2.12.



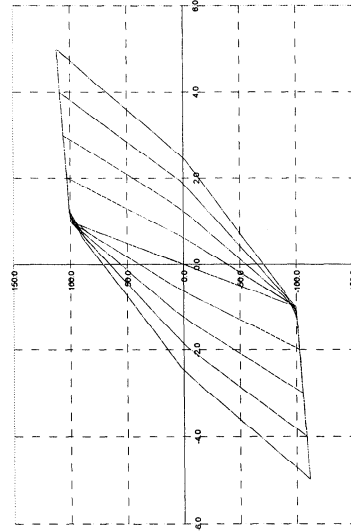
(a) Bilinear



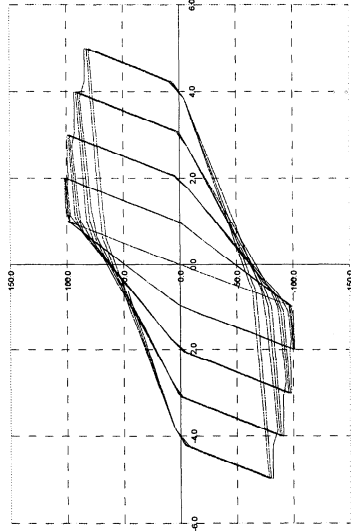
(b) Yield-oriented



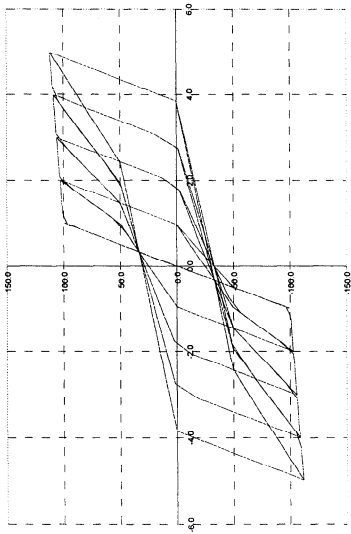
(c) Vertex-oriented



(d) Stiffness Degradation
($\alpha = 2$)



(e) Strength Degradation
($\beta_1 = 0.5, \beta_2 = 0.3, \mu_{ult} = 10$)



(f) Pinching
($\gamma = 0.5$)

Fig. 2.12 Examples of Hysteretic behavior modeled by the PHM

SECTION 3

THE SMOOTH HYSTERETIC MODEL (SHM)

The smooth model discussed here is a variation of the model originally proposed by Bouc (1967) and modified by several others (Wen, 1976, Baber and Noori, 1985, Casciati, 1989, Capecchi, 1991, Reinhorn et al, 1995, Madan et al, 1997). The derivation of this model from the theory of viscoplasticity and its resemblance with the endochronic constitutive theory are discussed in Section 4.

3.1 Plain Hysteretic Behavior without Degradation

Plain hysteretic behavior with post yielding hardening is modeled using two springs as shown in Fig. 3.1. When a moment is applied to the combination of springs, the two springs undergo the same deformation. However, springs share the applied moment in proportion to their instantaneous stiffnesses. The portion of the applied moment shared by the hysteretic spring is denoted by M^* .

3.1.1 Spring 1: Post-yield Spring

This is a linear elastic spring with the post-yielding stiffness of

$$K_{post-yield} = aK_0 \quad (3.1)$$

where K_0 = initial stiffness (elastic) and a = post-yielding to initial stiffness ratio.

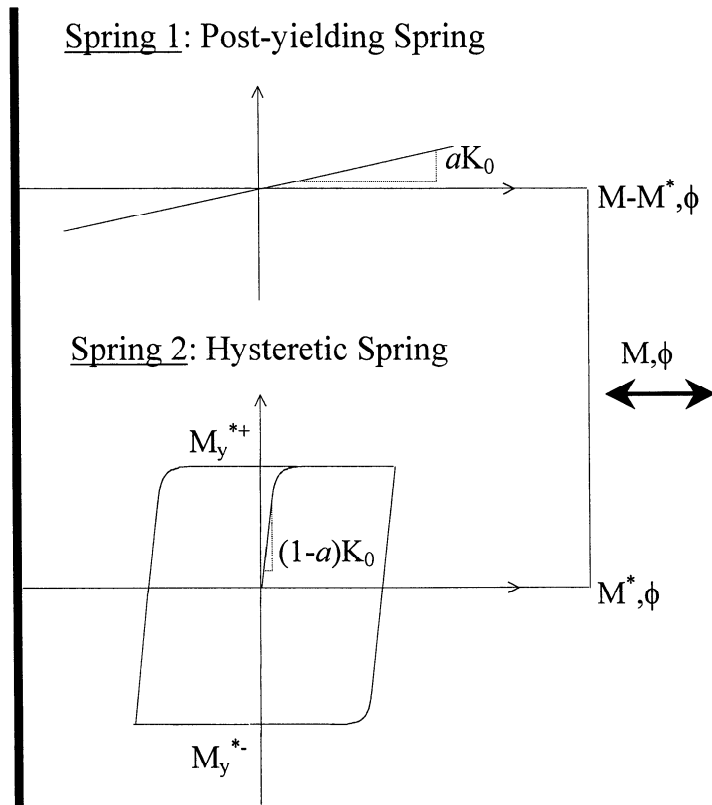


Fig. 3.1 Two-spring Model for Non-degrading Hysteretic Behavior

3.1.2 Spring 2: Hysteretic Spring

This is a pure elasto-plastic spring with a smooth transition from the elastic to the inelastic range. All degradation phenomena occur in this spring as will be described later in this section. The stiffness of this spring, when it is non-degrading is given by

$$K_{hysteretic} = (1-a)K_0 \left\{ 1 - \left| \frac{M^*}{M_y^*} \right|^N \left[\eta_1 \operatorname{sgn}(M^* \dot{\phi}) + \eta_2 \right] \right\} \quad (3.2)$$

where N = parameter controlling the smoothness of the transition from elastic to inelastic range, $\eta_1 = \eta$, a parameter controlling the shape of the unloading curve, $\eta_2 = 1 - \eta$,

$\phi_0 = \phi - \frac{M^*}{(1-a)K_0}$, M^* = portion of the applied moment shared by the hysteretic spring,

$M_y^* = (1-a)M_y$, the yield moment of the hysteretic spring and, sgn = the signum function. $\eta_1 + \eta_2 = 1$ for the model to be compatible with plasticity. This is discussed in Section 4.

Asymmetry can be introduced into the model by defining

$$M_y^* = (1-a) \left[\left(\frac{1 + \operatorname{sgn}(\dot{\phi})}{2} \right) M_y^+ + \left(\frac{1 - \operatorname{sgn}(\dot{\phi})}{2} \right) M_y^- \right] \quad (3.3)$$

where M_y^+ and M_y^- are the positive and negative yield moments respectively. The combined stiffness is given by,

$$K = K_{post-yield} + K_{hysteretic} \quad (3.4)$$

The SHM can now be represented as,

$$\dot{M} = K \dot{\phi} \quad (3.5)$$

3.2 Degradation

The stiffness and strength degradation rules for the SHM are the same as those for the PHM. They are however modified to fit the formulation of the SHM.

3.2.1 Stiffness Degradation

As mentioned earlier, stiffness degradation occurs only in the hysteretic spring. Thus the pivot rule is applied only to the hysteretic spring and the resulting hysteretic stiffness is given by,

$$K_{hysteretic} = (R_K - a)K_0 \left\{ 1 - \left| \frac{M^*}{M_y^*} \right|^N \left[\eta_1 \operatorname{sgn}(M^* \dot{\phi}) + \eta_2 \right] \right\} \quad (3.6)$$

where R_K = stiffness degradation factor given by equation (2.1).

3.2.2 Strength Degradation

The differential equations governing strength degradation in the SHM can be obtained by differentiating equation (2.3).

$$\frac{dM_y^{+/-}}{dt} = M_{y0}^{+/-} \left\{ \begin{aligned} & \left[1 - \frac{\beta_2}{1 - \beta_2} \frac{H}{H_{ult}} \right] \left[- \frac{1}{\beta_1 \left(\phi_u^{+/-} \right)^{\frac{1}{\beta_1}}} \left(\phi_{max}^{+/-} \right)^{\frac{1 - \beta_1}{\beta_1}} \right] \dot{\phi}_{max}^{+/-} \\ & + \left[1 - \left(\frac{\phi_{max}^{+/-}}{\phi_u^{+/-}} \right)^{\frac{1}{\beta_1}} \right] \left[- \frac{\beta_2}{(1 - \beta_2) H_{ult}} \right] \dot{H} \end{aligned} \right\} \quad (3.7a)$$

Writing equation (2.4) in the form of a differential equation, we have

$$\dot{H} = M \left(\dot{\phi} - \frac{\dot{M}}{R_K K_0} \right) = M \dot{\phi} \left[1 - \frac{(K_{post-yield} + R K_{hysteretic})}{R_K K_0} \right] \quad (3.7b)$$

The evolution equations for the maximum positive and negative curvatures can be written as

$$\dot{\phi}_{max}^+ = \dot{\phi} U(\phi - \phi_{max}^+) U(\dot{\phi}) \quad (3.7c)$$

$$\dot{\phi}_{max}^- = \dot{\phi} U(\phi_{max}^- - \phi) (1 - U(\dot{\phi})) \quad (3.7d)$$

where $U(x)$ is the heaviside step function. The differential equations (3.7a-d) govern strength degradation in the SHM. The solution of these equations will be discussed in Section 3.4.

3.2.3 Pinching or Slip

To model this effect, an additional spring called the slip-lock spring (Baber and Noori, 1985, Reinhorn et al, 1995) is added in series to the hysteretic spring. The

resulting combination is shown in Fig. 3.2. The stiffness of the slip-lock spring can be written as,

$$K_{Slip-Lock} = \left\{ \sqrt{\frac{2}{\pi}} \frac{s}{M_{\sigma}^*} \exp \left[-\frac{1}{2} \left(\frac{M^* - \bar{M}^*}{M_{\sigma}^*} \right)^2 \right] \right\}^{-1} \quad (3.8)$$

where $s = \text{slip length} = R_s (\phi_{\max}^+ - \phi_{\max}^-)$, $M_{\sigma}^* = \sigma M_y^*$, a measure of the moment range over which slip occurs, $\bar{M}^* = \lambda M_y^*$, the mean moment level on either side about which slip occurs, R_s , σ and λ are parameters of the model and ϕ_{\max}^+ and ϕ_{\max}^- are the maximum curvatures reached on the positive and negative sides respectively during the response. It is chosen to be a Gaussian type distribution so that, $\int_{-\infty}^{\infty} \frac{1}{K_{slip-lock}} dM = s$, the slip length. Any other convenient distribution fulfilling this condition could be chosen for the slip-lock flexibility.

The stiffness of the combined system is given by

$$K = K_{post-yield} + \frac{K_{Hysteretic} K_{slip-lock}}{K_{slip-lock} + K_{Hysteretic}} \quad (3.9)$$

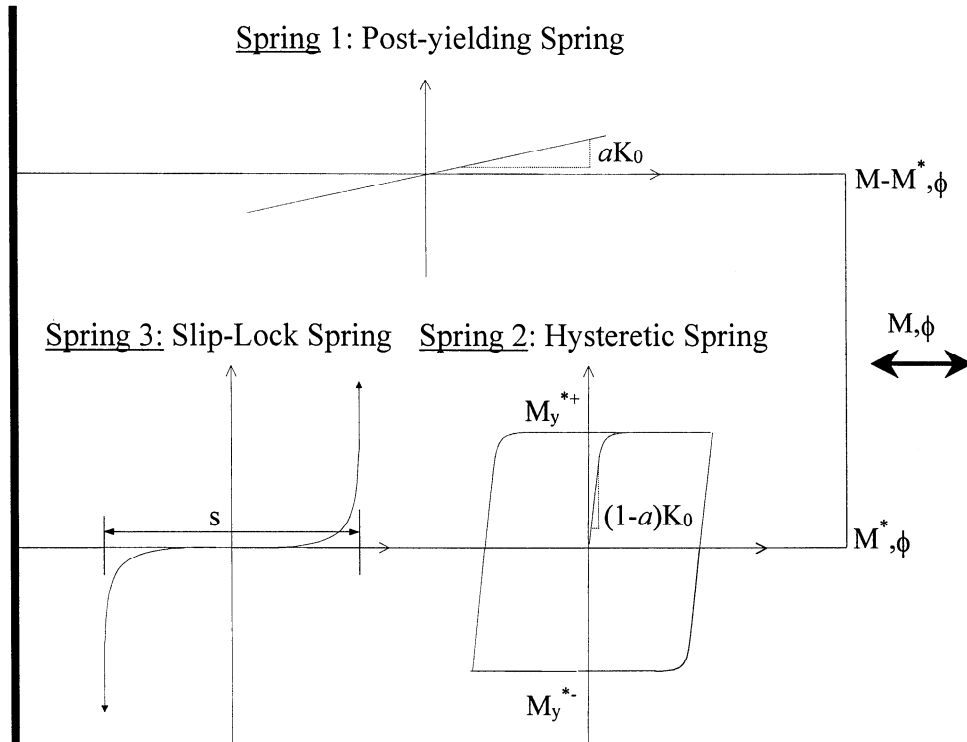


Fig. 3.2 Three-spring Model for Hysteretic Behavior with Slip

3.3 Gap Closing Behavior

Often, hysteretic elements exhibit stiffening under higher deformations. This happens for example in metallic dampers (Soong and Dargush, 1997) when axial behavior begins to predominate bending behavior and in bridge isolators (Reichman and Reinhorn, 1995, Priestley and Calvi, 1996) due to closing of the expansion gaps. Such behavior can be modeled by introducing an additional gap-closing spring in parallel as shown in Fig. 3.3. The moment in this spring and the stiffness of this spring are given by,

$$M^{**} = \kappa K_0 N_{gap} (|\phi| - \phi_{gap})^{N_{gap}-1} U(|\phi| - \phi_{gap}) \quad (3.10a)$$

$$K_{gap-closing} = \kappa K_0 N_{gap} (|\phi| - \phi_{gap})^{N_{gap}-1} U(|\phi| - \phi_{gap}) \quad (3.10b)$$

where M^{**} = moment in the gap-closing spring, $K_{gap-closing}$ = stiffness of the gap-closing spring, ϕ_{gap} = gap-closing curvature, U = heaviside step function and κ and N_{gap} are parameters.

3.4 Solution of the SHM

There are two possible approaches to solving the equations governing the SHM – (i) The conventional incremental approach and (ii) the State-Space Approach (SSA) (Simeonov et al, 1999). Equations (3.5) and (3.7) can be used directly in the latter solution approach. However, only the former approach will be discussed here. For this purpose, equations (3.5) and (3.7) have to be written in time-independent form. Also, since the post-yielding and gap-closing springs are algebraic, only the hysteretic and slip-

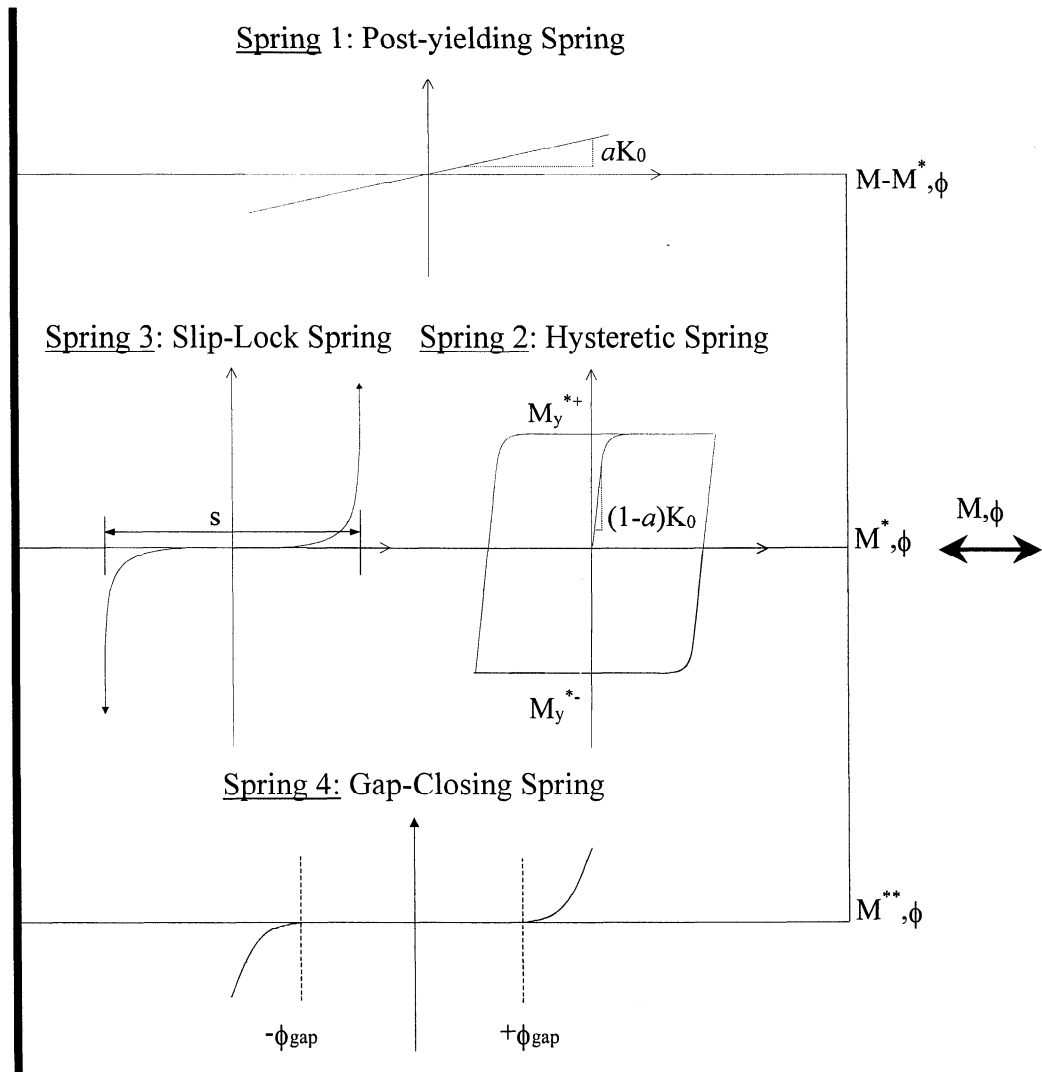


Fig. 3.3 Gap-Closing Spring in Parallel

lock springs are solved and the results added. This results in the following time-independent differential equations within a global time step:

$$\frac{dM^*}{d\phi} = \frac{K_{Hysteretic}K_{slip-lock}}{K_{slip-lock} + K_{Hysteretic}} \quad (3.11a)$$

$$\frac{dM_y^{*+}}{d\phi} = M_y^{*0+} \left\{ \begin{aligned} & \left[1 - \frac{\beta_2}{1-\beta_2} \frac{H}{H_{ult}} \right] \left[-\frac{1}{\beta_1 \left(\phi_u^+\right)^{\frac{1}{\beta_1}}} \left(\phi_{max}^+\right)^{\frac{1-\beta_1}{\beta_1}} \right] U(\phi - \phi_{max}^+) U(\Delta\phi) \\ & + \left[1 - \left(\frac{\phi_{max}^+}{\phi_u^+}\right)^{\frac{1}{\beta_1}} \right] \left[-\frac{\beta_2}{1-\beta_2} \frac{1}{H_{ult}} \right] M^* \left[1 - \frac{1}{(1-a)R_K K_0} \frac{K_{Hysteretic}K_{slip-lock}}{K_{slip-lock} + K_{Hysteretic}} \right] \end{aligned} \right\} \quad (3.11b)$$

$$\frac{dM_y^{*-}}{d\phi} = M_y^{*0-} \left\{ \begin{aligned} & \left[1 - \frac{\beta_2}{1-\beta_2} \frac{H}{H_{ult}} \right] \left[-\frac{1}{\beta_1 \left(\phi_u^-\right)^{\frac{1}{\beta_1}}} \left(\phi_{max}^-\right)^{\frac{1-\beta_1}{\beta_1}} \right] U(\phi_{max}^- - \phi) [1 - U(\Delta\phi)] \\ & + \left[1 - \left(\frac{\phi_{max}^-}{\phi_u^-}\right)^{\frac{1}{\beta_1}} \right] \left[-\frac{\beta_2}{1-\beta_2} \frac{1}{H_{ult}} \right] M^* \left[1 - \frac{1}{(1-a)R_K K_0} \frac{K_{Hysteretic}K_{slip-lock}}{K_{slip-lock} + K_{Hysteretic}} \right] \end{aligned} \right\} \quad (3.11c)$$

$$\frac{d\phi_{max}^+}{d\phi} = U(\phi - \phi_{max}^+) U(\Delta\phi) \quad (3.11d)$$

$$\frac{d\phi_{max}^-}{d\phi} = U(\phi_{max}^- - \phi) [1 - U(\Delta\phi)] \quad (3.11e)$$

$$\frac{dH}{d\phi} = M^* \left[1 - \frac{1}{(1-a)R_K K_0} \frac{K_{Hysteretic}K_{slip-lock}}{K_{slip-lock} + K_{Hysteretic}} \right] \quad (3.11f)$$

Equations 3.11 can be solved within each global integration step using any method such as the adaptive RK45 or the Semi-implicit Rosenbrock methods (Nagarajaiah et al, 1989, Press et al, 1992). The latter require the Jacobian of equations 3.11 for Newton-Raphson iterations. Since it is quite cumbersome to develop the exact Jacobian, it is derived using two assumptions – the slip-lock element is not considered and the change of the stiffness degradation factor with deformation is neglected. Since the Jacobian is only an iteration matrix, these approximations do not cause any error in the solution. The resulting non-zero components of the 6x6 Jacobian are listed below:

$$J(1,1) = -(1-a)K_0 \left\{ \left[\eta_1 \operatorname{sgn}(M^* \Delta\phi + \eta_2) \right] \frac{|M^*|^{N-1}}{|M_y^*|^N} \operatorname{sgn}\left(\frac{M^*}{M_y^*}\right) \right\} \quad (3.12a)$$

$$J(1,2) = \left[\frac{1 + \operatorname{sgn}(\Delta\phi)}{2} \right] \left\{ N(1-a)K_0 \left[\eta_1 \operatorname{sgn}(M^* \Delta\phi + \eta_2) \right] \frac{|M^*|^N}{|M_y^{*+}|^{N+1}} \right\} \quad (3.12b)$$

$$J(1,3) = -\left[\frac{1 - \operatorname{sgn}(\Delta\phi)}{2} \right] \left\{ N(1-a)K_0 \left[\eta_1 \operatorname{sgn}(M^* \Delta\phi + \eta_2) \right] \frac{|M^*|^N}{|M_y^{*-}|^{N+1}} \right\} \quad (3.12c)$$

$$J(2,1) = M_y^{*0+} \left[1 - \left(\frac{\phi_{\max}^+}{\phi_u^+} \right)^{\frac{1}{\beta_1}} \left[-\frac{\beta_2}{(1-\beta_2)H_{ult}} \right] \right. \\ \left. \left\{ \left[1 - \frac{K_{Hysteretic}}{(1-a)R_K K_0} \right] - M^* \frac{J(1,1)}{(1-a)R_K K_0} \right\} \right] \quad (3.12d)$$

$$J(2,4) = M_y^{*0+} \left\{ \begin{aligned} & \left[1 - \frac{\beta_2 H}{(1-\beta_2)H_{ult}} \right] U(\phi - \phi_{\max}^+) U(\Delta\phi) \left[-\frac{1-\beta_1}{\beta_1^2 (\phi_u^+)^{\frac{1}{\beta_1}}} (\phi_{\max}^+)^{\frac{1-2\beta_1}{\beta_1}} \right] \\ & + M^* \left[\frac{\beta_2}{(1-\beta_2)H_{ult}} \right] \left[\frac{1}{\beta_1 (\phi_u^+)^{\frac{1}{\beta_1}}} (\phi_{\max}^+)^{\frac{1-\beta_1}{\beta_1}} \right] U(\phi - \phi_{\max}^+) U(\Delta\phi) \end{aligned} \right\} \quad (3.12e)$$

$$J(2,6) = M_y^{*0+} \left[\frac{\beta_2}{(1-\beta_2)H_{ult}} \right] \left[\frac{1}{\beta_1 (\phi_u^+)^{\frac{1}{\beta_1}}} (\phi_{\max}^+)^{\frac{1-\beta_1}{\beta_1}} \right] U(\phi - \phi_{\max}^+) U(\Delta\phi) \quad (3.12f)$$

$$J(3,1) = M_y^{*0-} \left[1 - \left(\frac{\phi_{\max}^-}{\phi_u^-} \right)^{\frac{1}{\beta_1}} \right] \left[-\frac{\beta_2}{(1-\beta_2)H_{ult}} \right] \quad (3.12g)$$

$$\left\{ \left[1 - \frac{K_{Hysteretic}}{(1-a)R_K K_0} \right] - M^* \frac{J(1,1)}{(1-a)R_K K_0} \right\}$$

$$J(3,5) = M_y^{*0-} \left\{ \begin{aligned} & \left[1 - \frac{\beta_2 H}{(1-\beta_2)H_{ult}} \right] U(\phi_{\max}^- - \phi) [1 - U(\Delta\phi)] \left[-\frac{1-\beta_1}{\beta_1^2 |\phi_u^-|^{\frac{1}{\beta_1}}} |\phi_{\max}^-|^{\frac{1-2\beta_1}{\beta_1}} \right] \\ & + M^* \left[\frac{\beta_2}{(1-\beta_2)H_{ult}} \right] \left[\frac{1}{\beta_1 |\phi_u^-|^{\frac{1}{\beta_1}}} |\phi_{\max}^-|^{\frac{1-\beta_1}{\beta_1}} \right] U(\phi_{\max}^- - \phi) [1 - U(\Delta\phi)] \end{aligned} \right\} \quad (3.12h)$$

$$J(3,6) = M_y^{*0-} \left[\frac{\beta_2}{(1-\beta_2)H_{ult}} \right] \left[\frac{1}{\beta_1 |\phi_u^-|^{\frac{1}{\beta_1}}} |\phi_{\max}^-|^{\frac{1-\beta_1}{\beta_1}} \right] U(\phi_{\max}^- - \phi) [1 - U(\Delta\phi)] \quad (3.12i)$$

$$J(6,1) = \left[1 - \frac{K_{Hysteretic}}{(1-a)R_K K_0} \right] - M^* \frac{J(1,1)}{(1-a)R_K K_0} \quad (3.12j)$$

3.5 Examples

Examples of various types of hysteretic behavior modeled by the SHM are shown in Fig. 3.4. Ranges of degradation parameters obtained from experimental results of the SAC Joint Venture (1996) are shown in Table 3.1. Moreover, comparison between behavior predicted by the SHM and these experimental results is presented in Table 3.2.

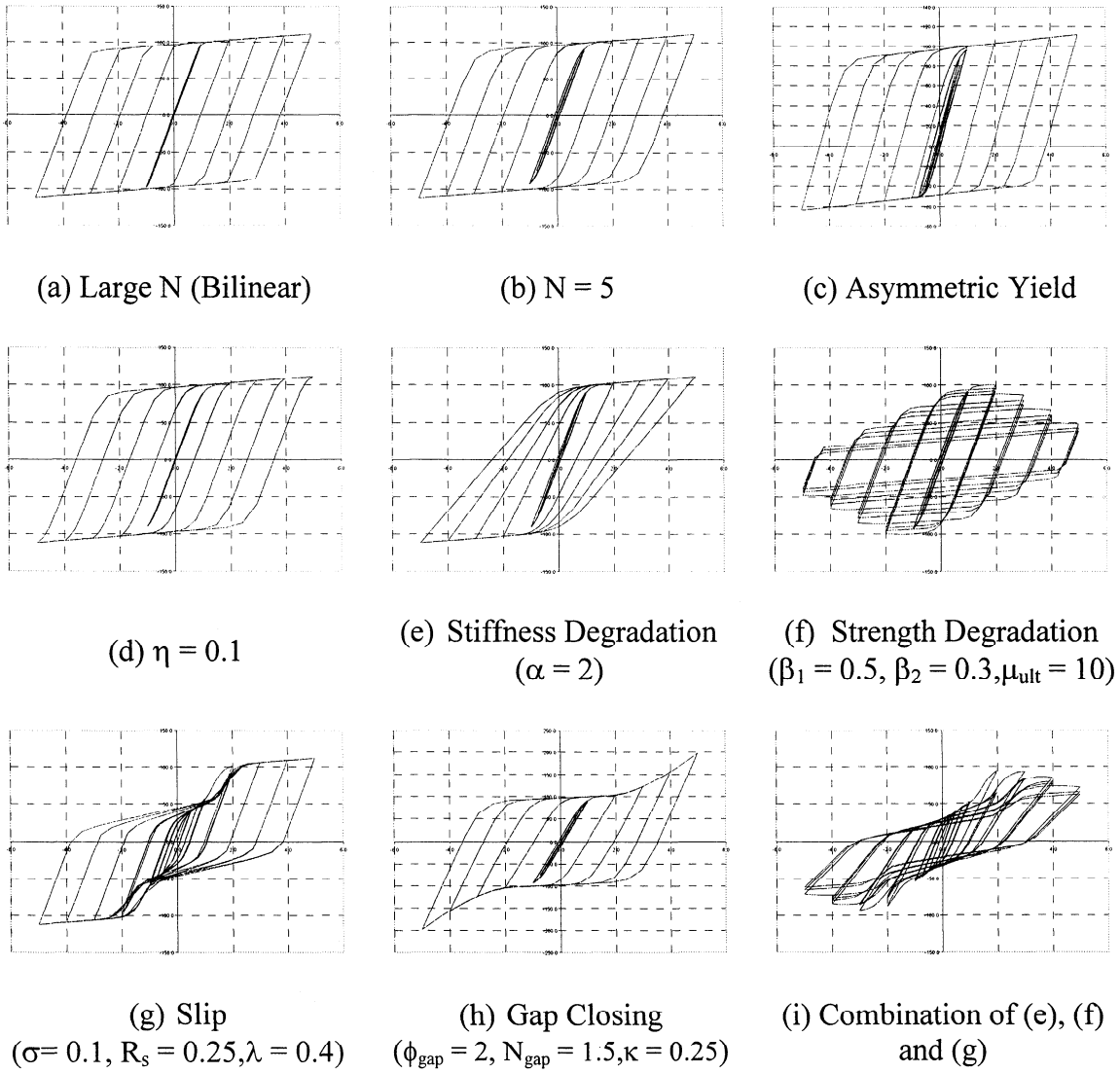


Fig. 3.4 Examples of Hysteretic Behavior Modeled by the SHM

Table 3.1 Range of Parameters

	Mild	Moderate	Severe
α	15	10	4
β_1	0.00	0.30	0.60
β_2	0.00	0.15	0.30

Table 3.2 Results from Connection Tests (SAC Joint Venture, 1996)

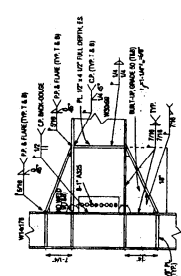
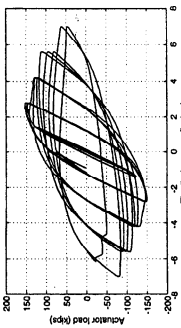
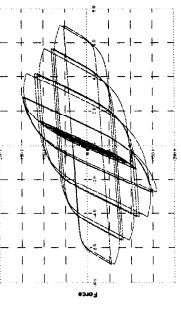
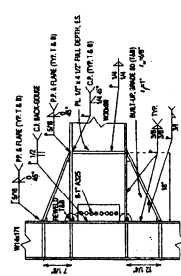
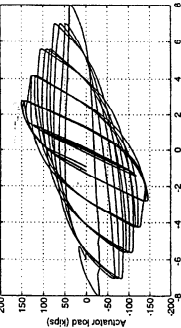
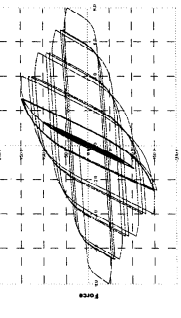
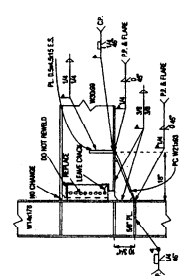
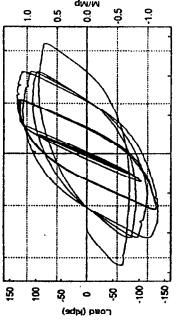
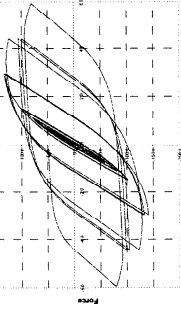
SPECIMEN NAME	DETAIL	FEATURES	EXPERIMENTAL RESPONSE	ANALYTICAL RESPONSE	PARAMETERS
EERC-RN2		Top and bottom triangular haunch, Beam flange not welded, Flange local buckling, Web Distortion			α 1.0 β_1 0.50 β_2 0.25 μ_{ult} 9.0
EERC-RN3		Top and bottom triangular haunch, Beam flange not welded, Flange local buckling, Web Distortion			α 1.0 β_1 0.60 β_2 0.30 μ_{ult} 8.0
UCSD-1R		Bottom Haunch, Unconnected beam bottom flange, Local and lateral torsional buckling, Haunch yielding			α 5 β_1 0.40 β_2 0.20 μ_{ult} 7.1

Table 3.2 Results from Connection Tests (SAC Joint Venture, 1996) (contd.)

SPECIMEN NAME	DETAIL	FEATURES	EXPERIMENTAL RESPONSE	ANALYTICAL RESPONSE	PARAMETERS
UCSD-2R		Replacement plate for beam top flange, Shear tab to column weld, Web buckling, Flange fracture			α 10 β_1 0.00 β_2 0.15 μ_{ult} 8.0
UCSD-3R		Replacement top plate, Bottom triangular haunch, Beam to column weld, Local buckling			α 15 β_1 0.60 β_2 0.15 μ_{ult} 7.6
UTA-1R		Bottom triangular haunch, Beam and column splice plates, Web doubler plates, Flange and web yielding, Top weld fracture			α 5 β_1 0.10 β_2 0.10 μ_{ult} 9.6

Table 3.2 Results from Connection Tests (SAC Joint Venture, 1996) (contd.)

SPECIMEN NAME	DETAIL	FEATURES	EXPERIMENTAL RESPONSE	ANALYTICAL RESPONSE	PARAMETERS
UTA-3R		<p>Top and bottom triangular haunch, Web doubler plate, Flange and web buckling, Specimen twisting</p>			α 4
			β_1 0.20		
			β_2 0.30		
			μ_{ult} 5.6		
EERC-AN1		<p>Top and bottom cover plates, Notch tough weld material, Local buckling, Fillet weld crack, Net section Fracture</p>			α 5
			β_1 0.00		
			β_2 0.10		
			μ_{ult} 6.0		
UTA-4		<p>Top and bottom cover plates, Notch tough weld material, Local buckling, Fillet weld crack, Specimen twisting</p>			α 5
			β_1 0.05		
			β_2 0.15		
			μ_{ult} 10.0		

SECTION 4

UNIFICATION OF CONCEPTS FOR REPRESENTATION OF INELASTIC MATERIAL BEHAVIOR IN ONE DIMENSION

4.1 Background

An elastic body is one in which the strain at any point is completely determined by the current stress and temperature. This dependence on current stress and temperature is not arbitrary. The *principle of state* of classical equilibrium thermodynamics (see for example Moran and Shapiro, 1995) states that the state of a system undergoing a reversible process is completely determined by one variable characterizing heat transfer (temperature) and one variable for each mode in which the system can transfer work (stress). It can be shown (see for example Fung, 1965) that when a process undergone by an elastic body is adiabatic, the strain energy is the internal energy, that when the process is isothermal, the strain energy is the Helmholtz free energy function, and that in either case, its partial derivatives with respect to strain are independent of temperature. It can then be reasonably assumed that most processes of engineering structures are isothermal, thus excluding temperature from the analysis. When this is not true, additional constitutive equations involving temperature are required.

The obvious definition of an inelastic body is then, as one in which there is “something else”, besides current stress and temperature that determines strain. The task of developing inelastic constitutive models is therefore describing this “something else”. Fig. 4.6 shows a schematic of several ways of doing this and how they are related to each

other. When a material starts behaving inelastically, it departs from the realm of classical equilibrium thermodynamics. The theory of irreversible thermodynamics must be applied. Since the principle of state does not hold anymore, it can be *postulated* that there exist a number of additional “internal” or “hidden” state variables. In the macroscopic sense, these variables may for example be yield moment, maximum attained curvature, etc. The rigorous background to the internal state variable (ISV) theory of irreversible thermodynamics of inelastic materials was established by Coleman and Gurtin (1967) using the theory of nonlinear differential equations. The ISV formulation may be written as,

$$\dot{\sigma} = f(\varepsilon, \dot{\varepsilon}, \boldsymbol{\xi}) \text{ and } \dot{\boldsymbol{\xi}} = g(\varepsilon, \dot{\varepsilon}, \boldsymbol{\xi}) \quad (4.1a)$$

or

$$\dot{\varepsilon} = f(\sigma, \dot{\sigma}, \boldsymbol{\xi}) \text{ and } \dot{\boldsymbol{\xi}} = g(\sigma, \dot{\sigma}, \boldsymbol{\xi}) \quad (4.1b)$$

where ε = strain, σ = stress, $\boldsymbol{\xi}$ = vector of ISV's and “ $\dot{\cdot}$ ” denotes differentiation with respect to time. Nelson and Dorfmann (1995) characterize equations of type (4.1a) as parallel plasticity models and those of type (4.1b) as series plasticity models.

Biot (1954) used the ISV theory for a linear hereditary material (linear viscoelastic) for which the Onsager reciprocal principle (Fung, 1965) holds. His formulation showed that a general anisotropic linear dissipative material can be

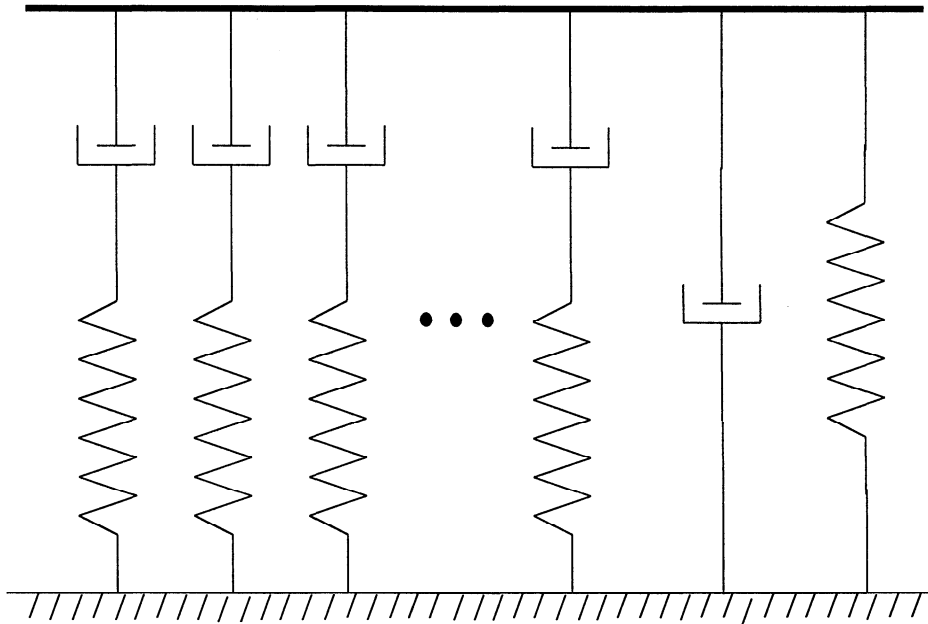


Fig. 4.1 Spring and Dashpot Representation of Linear Viscoelastic Material

visualized as a combination of springs and dashpots (Fung, 1965) as shown in Fig. 4.1. A similar derivation of a general viscoplastic model from the principles of irreversible thermodynamics has been done by many researchers (for example, Freed et al, 1991 and Ristinmaa, 1999). This is however much more involved because the Onsager reciprocal principle is no longer valid.

The “something else” may otherwise be thought of as the past history of stress. The past history may be defined precisely using concepts of functional analysis and a highly mathematical theory known as the *theory of materials with memory* has been created to deal with it (Coleman, 1964). In simple terms, this may be represented as,

$$\sigma(t) = \underset{s=-\infty}{\overset{t}{\Xi}} \varepsilon(s) \text{ or } \varepsilon(t) = \underset{s=-\infty}{\overset{t}{\Xi}} \sigma(s) \quad (4.2)$$

where Ξ is a functional. This kind of material description is very difficult to work with and therefore, the constitutive theories based on ISV's are in more popular use. It can be shown however (Lubliner, 1969) that under certain conditions, the ISV theory is a first order approximation to the theory of materials with memory.

Yet another way of describing inelastic behavior is to define the evolution of ISV's by physically motivated rules rather than by differential equations. The equivalence of these two approaches was demonstrated by Ziaming and Katukura (1990) and is discussed later. In the following paragraphs, several hysteretic models are considered and the relationships between them are discussed in the context of the theory described thus far.

4.2 Algebraic Models

4.2.1 Masing's Hypothesis (Beck and Jayakumar, 1996)

If the virgin loading curve is given by an algebraic relationship,

$$f(\phi, M) = 0 \quad (4.3a)$$

then according to Masing's Hypothesis, the curve between the points $(\phi_{vertex}^+, M_{vertex}^+)$ and $(\phi_{vertex}^-, M_{vertex}^-)$ is given by,

$$f\left(\frac{M - M_{vertex}}{2}, \frac{\phi - \phi_{vertex}}{2}\right) = 0 \quad (4.3b)$$

where

$$M_{vertex} = \left(\frac{1 + \text{sgn}(\Delta\phi)}{2}\right)M_{vertex}^+ + \left(\frac{1 - \text{sgn}(\Delta\phi)}{2}\right)M_{vertex}^- \quad (4.3c)$$

$$\phi_{vertex} = \left(\frac{1 + \text{sgn}(\Delta\phi)}{2}\right)\phi_{vertex}^+ + \left(\frac{1 - \text{sgn}(\Delta\phi)}{2}\right)\phi_{vertex}^- \quad (4.3d)$$

4.2.2 Ramberg-Osgood Model

One such algebraic virgin curve that can be used in conjunction with Masing's Hypothesis to create a hysteretic model is the Ramberg-Osgood Model (Ramberg and Osgood, 1943) given by,

$$\frac{\phi}{\phi_y} = \frac{M}{M_y} + \eta \left(\frac{M}{M_y} \right)^N \quad (4.4)$$

where η (positive) and N (odd integer) are parameters of the model. It will be shown later that hysteretic models based on differential equations, that exhibit smooth virgin curves generally exhibit local violation of Drucker's Stability Postulate (Thyagarajan, 1989). Although the algebraic model discussed here exhibits a smooth virgin curve, it does not violate Drucker's Stability Postulate. However its implementation is extremely involved. The model resembles the theory of materials with memory. The Menegotto-Pinto equation (Gomes and Julio, 1997) is another virgin stress-strain relationship that can be used in conjunction with Masing's Hypothesis.

4.3 Differential Equation Models

4.3.1 Plasticity Based on Yield Surface

According to this theory, there is a distinct boundary in stress-space, which separates the elastic and inelastic (plastic) states of the material. In three-dimensional stress-space, this boundary is called the yield-surface. The theory of plasticity based on a yield-surface is discussed in detail, for example, by Malvern (1969) and Lubliner (1990). In one dimension, however, this surface reduces to positive and negative yield points. The resulting constitutive equation is given by (Ziaming and Katukura, 1990),

$$\dot{M} = \dot{\phi}KU(\dot{\phi})U(M)U(M_y^+ - M) + \dot{\phi}KU(\dot{\phi})U(-M) + \dot{\phi}KU(-\dot{\phi})U(M) + \dot{\phi}KU(-\dot{\phi})U(-M)U(-M_y^- + M) \quad (4.5a)$$

or

$$\dot{M} = K \left[1 - U(\dot{\phi})U(M - M_y^+) - U(-\dot{\phi})U(-M + M_y^-) \right] \dot{\phi} \quad (4.5b)$$

or

$$\dot{M} = K \left[1 - \frac{1 + \text{sgn}(M\dot{\phi})}{2} \{ U(M_y^+ - M)U(M) + U(-M_y^- + M)U(-M) \} \right] \dot{\phi} \quad (4.5c)$$

Equations 4.5a, b and c can be shown to be exactly equivalent. However 4.5a represents the loading and unloading contributions explicitly and this is useful in the integral formulation of the infinite spring-slider model discussed later.

4.3.2 Plasticity/Viscoplasticity without a Yield Surface

According to Bodner (1968), “yielding is not a separate and independent criterion but is a consequence of a general constitutive law of the material behavior”. Several constitutive models for both rate-dependent (viscoplastic) and rate-independent (plastic) inelastic behavior have been derived without a formal hypothesis of a yield surface. Three such models are discussed here – the Endochronic Model, the Ozdemir Model and the Wen-Bouc Model. Each of them was conceived based on a different motivation. Nevertheless, it is shown that they exhibit similar behavior and become identical under certain limiting conditions.

4.3.3 Endochronic Theory

The endochronic theory was first proposed by Valanis (1971,1980). The basic concept is that of an *intrinsic time* that is related to the deformation history of the material, the relation itself being a material property. An *intrinsic time measure* in the general three-dimensional case is defined for example by,

$$d\zeta^2 = A_{ijkl} d\varepsilon_{ij}^i d\varepsilon_{kl}^i + B^2 dt^2 \quad (4.6a)$$

where A and B are material properties and ε^i denotes the plastic component of strain. $B = 0$ describes rate independent (plastic) behavior. An intrinsic time scale is next defined as $z(\zeta)$, a monotonically increasing function. This is then substituted for real time in the convolution integral of linear viscoelasticity. For the uniaxial case, this results in,

$$\sigma = \int_0^z R(z - z') \frac{d\varepsilon}{dz} dz' \quad (4.6b)$$

Bazant (1976) provides a more physical interpretation of the endochronic theory for the uniaxial case starting from the Maxwell model and replacing real time by a function of plastic strain. The resulting model is given by,

$$\dot{M} = K_0 \dot{\phi} - \frac{1}{Z} M |\dot{\phi}| \quad (4.7)$$

where $Z = M_y/K_0$

4.3.4 Ozdemir Model (Ozdemir, 1976)

Consider the force displacement relationship for a linear damper (Fig. 4.2a):

$$M = c\dot{\phi} \quad (4.8)$$

The steady-state force-displacement relationship is shown in Fig. 4.2b. Consider this damper being made nonlinear as follows:

$$M = c\dot{\phi}^{\frac{1}{N}} \text{ or } \dot{\phi} = \frac{1}{c}M^N \quad (4.9)$$

where N is an odd integer to preserve signs. The force displacement relationship of such a damper is shown in Fig. 4.2d. It is seen that as N tends to ∞ , the behavior of the damper tends to a slider. Adding a spring in series to form a Maxwell element with a nonlinear damper results in,

$$\dot{\phi} = \frac{\dot{M}}{K_0} + \frac{1}{c}M^N \quad (4.10a)$$

Rewriting this results in Ozdemir's rate-dependent model:

$$\frac{\dot{\phi}}{\phi_y} = \frac{\dot{M}}{M_y} + \frac{1}{\tau} \left(\frac{M}{M_y} \right)^N \text{ or } \frac{\dot{M}}{M_y} = \frac{\dot{\phi}}{\phi_y} - \frac{1}{\tau} \left(\frac{M}{M_y} \right)^N \quad (4.10b)$$

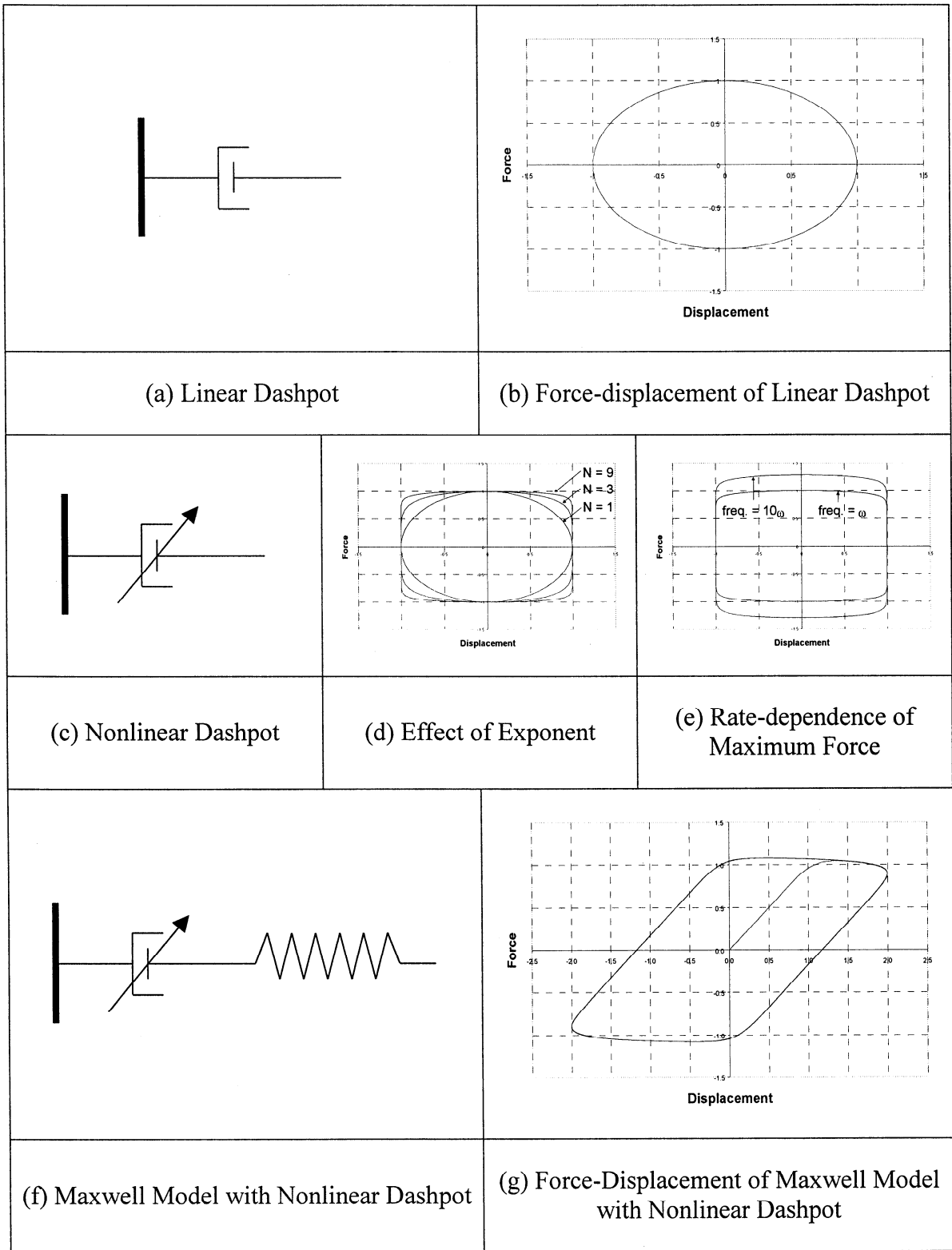


Fig. 4.2 Development of Ozdemir's Model

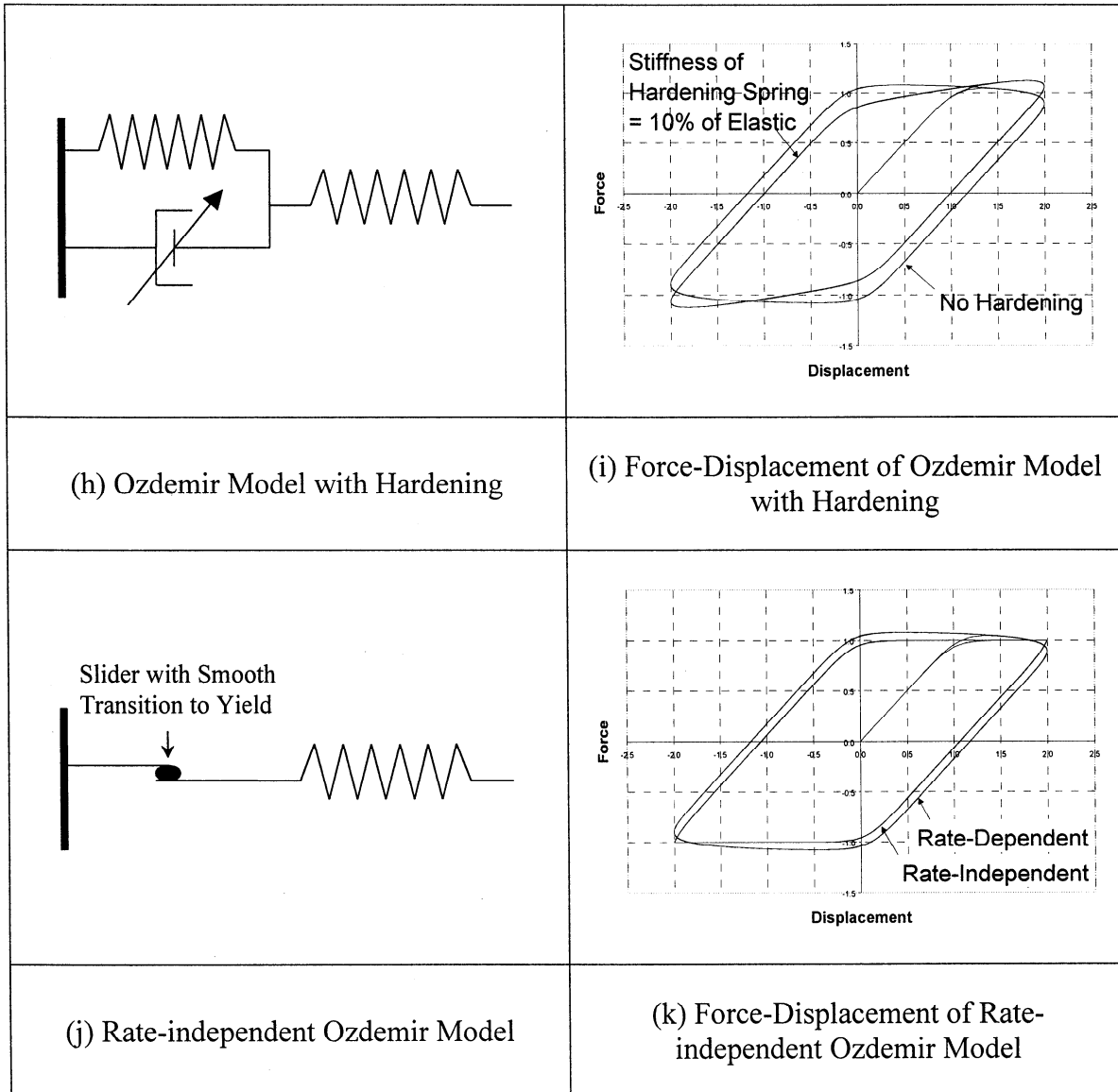


Fig. 4.2 Development of Ozdemir's Model

where $\tau = cM_y^{\frac{1}{N}} = \phi_y$ = the time constant. As $N \rightarrow \infty$, the model approaches an elastoplastic model. However, the yield strength is rate-dependent. It could be moderate-independent, by making the yield strength a function of the loading or by making N a function of the rate of loading. Ozdemir (1976) discusses these possibilities. But neither of these is a general solution. The alternate solution provided by Ozdemir is to make the time-constant a function of strain rate. It can be shown that there exists a time-constant τ for each loading rate $\dot{\phi}$ that makes the model rate independent. We therefore define

$\tau = \left| \frac{\dot{\phi}}{\phi_y} \right|$. The rate-independent Ozdemir model is then,

$$\frac{\dot{M}}{M_y} = \frac{\dot{\phi}}{\phi_y} - \left| \frac{\dot{\phi}}{\phi_y} \right| \left(\frac{M}{M_y} \right)^N \quad (4.10c)$$

The nonlinear dashpot can now be replaced by a slider (Fig. 4.2j) and the resulting force-displacement relationship is shown in Fig. 4.2k. Ozdemir also suggests an alternative interpretation.

Consider equation (4.10b) to be governed by a material time T rather than the inertial time t . Then,

$$\frac{d}{dT} \left(\frac{M}{M_y} \right) = \frac{d}{dT} \left(\frac{\phi}{\phi_y} \right) - \frac{1}{\tau} \left(\frac{M}{M_y} \right)^N \quad \text{or} \quad \frac{d}{dt} \left(\frac{M}{M_y} \right) \frac{dt}{dT} = \frac{d}{dt} \left(\frac{\phi}{\phi_y} \right) \frac{dt}{dT} - \frac{1}{\tau} \left(\frac{M}{M_y} \right)^N \quad (4.11a)$$

$$\frac{\dot{M}}{M_y} = \frac{\dot{\phi}}{\phi_y} - \frac{1}{\tau} \frac{dT}{dt} \left(\frac{M}{M_y} \right)^N \quad (4.11b)$$

Comparing (4.11b) with (4.10c), we have,

$$\frac{1}{\tau} \frac{dT}{dt} = \frac{1}{|\phi_y|} \frac{d|\phi|}{dt} \text{ or } dT = \frac{\tau}{|\phi_y|} d|\phi| \quad (4.11c)$$

where T is now similar to the intrinsic time of Bazant and Valanis.

Hardening may be introduced into the model by adding a linear hardening spring in parallel with the nonlinear dashpot as shown in Fig. 4.2h. The force in this spring is referred to as the back-stress S . The final equation with hardening (rate-dependent form) is given by,

$$\frac{\dot{M}}{M_y} = \frac{\dot{\phi}}{\phi_y} - \frac{1}{\tau} \left(\frac{M - S}{M_y} \right)^N \quad (4.10d)$$

The resulting force-displacement relationship is shown in Fig. 4.2i.

4.3.5 Wen-Bouc Model

Only the hysteretic component is considered in this model. Bouc (1967) and Wen (1976), using some mathematical reasoning came up with the following equation (reformulated by Reinhorn et al, 1995).

$$\dot{M} = K \left\{ 1 - \left| \frac{M}{M_y} \right|^N [\eta_1 \operatorname{sgn}(M \dot{\phi}) + \eta_2] \right\} \dot{\phi} \quad (4.12)$$

It can be shown however that this equation can be derived from the equations of one-dimensional plasticity based on a surface, equation 4.5b, by smoothening the heaviside step function as follows.

$$\dot{M} = K \left[1 - \frac{1 + \operatorname{sgn}(M \dot{\phi})}{2} \{ U(M_y^+ - M) U(M) + U(-M_y^- + M) U(-M) \} \right] \dot{\phi} \quad (4.5c)$$

Assuming for simplicity that $M_y^+ = -M_y^- = |M_y|$, we have,

$$\dot{M} = K \left[1 - \frac{1 + \operatorname{sgn}(M \dot{\phi})}{2} U(|M_y| - |M|) \right] \dot{\phi} \quad (4.13)$$

The heaviside step function can be smoothened as follows:

$$U(|M_y| - |M|) \approx \left| \frac{M}{M_y} \right|^N \quad (4.14)$$

The two are exactly equal when $N \rightarrow \infty$. Substituting (4.14) in (4.13) leads to the special case of (4.12) for which $\eta_1 = \eta_2 = 0.5$. From (4.12),

$$\frac{dM}{d\phi} = K \left\{ 1 - \left| \frac{M}{M_y} \right|^N [\eta_1 \operatorname{sgn}(M \dot{\phi}) + \eta_2] \right\}$$

In the case of monotonic loading in the positive direction,

$$\frac{dM}{d\phi} = K \left\{ 1 - \left| \frac{M}{M_y} \right|^N [\eta_1 + \eta_2] \right\}$$

When M is a maximum, $\frac{dM}{d\phi} = 0$, i.e.,

$$1 - \left| \frac{M_{\max}}{M_y} \right|^N [\eta_1 + \eta_2] = 0$$

$$M_{\max} = M_y \left(\frac{1}{\eta_1 + \eta_2} \right)^{\frac{1}{N}}$$

Therefore $\eta_1 + \eta_2 = 1$ always (Constantinou and Adnane, 1987). A more general derivation of the relationship between a three-dimensional Wen-Bouc model and a plasticity model based on a yield function is given by Casciati (1989). Let us now consider two limiting cases of the Wen-Bouc model.

Case(i) $\eta_1 = 1; \eta_2 = 0$:

$$\dot{M} = K \left\{ 1 - \left| \frac{M}{M_y} \right|^N \operatorname{sgn}(M \dot{\phi}) \right\} \dot{\phi} = K \left\{ 1 - \left| \frac{M}{M_y} \right|^N \operatorname{sgn}(M) \operatorname{sgn}(\dot{\phi}) \right\} \dot{\phi}$$

If N is an odd integer, then,

$$\dot{M} = K \left\{ 1 - \left(\frac{M}{M_y} \right)^N \text{sgn}(\dot{\phi}) \right\} \dot{\phi} = K \left\{ \dot{\phi} - \left| \dot{\phi} \right| \left(\frac{M}{M_y} \right)^N \right\}, \text{ i.e.,}$$

$$\frac{\dot{M}}{M_y} = \frac{\dot{\phi}}{\phi_y} - \left| \frac{\dot{\phi}}{\phi_y} \right| \left(\frac{M}{M_y} \right)^N \text{ which is exactly the Ozdemir model of equation 4.10d.}$$

Case(ii) $\eta_1=0$; $\eta_2 = 1$:

$$\dot{M} = K \left\{ 1 - \left| \frac{M}{M_y} \right|^N \right\} \dot{\phi}, \text{ i.e.,}$$

$$\phi = \frac{M}{K} \frac{1}{\left\{ 1 - \left| \frac{M}{M_y} \right|^N \right\}}$$

which is the Menegotto-Pinto equation for nonlinear elastic behavior. The Wen-Bouc model can therefore be thought of as a weighted combination of the rate-independent Ozdemir model and the nonlinear elastic Menegotto-Pinto model, which produces a smooth elasto-plastic model for the particular weight set, $\eta_1 = \eta_2 = 0.5$.

4.3.6 Spring and Slider models

Biot's thermodynamic formulation for a linear dissipative material when interpreted physically leads to a parallel combination of Maxwell models. Ozdemir's model suggests that a Maxwell model can be generalized with a nonlinear dashpot, which

in the limit leads to an elasto-plastic model. These factors motivate us to consider models that are combinations of springs and sliders as shown in Fig. 4.3. The Distributed Element Model (DEM) of Iwan (1966) and Thyagarajan (1989) belong to this class. Jayakumar (1987) shown that in the limit of infinite springs and sliders, this model leads to cyclic algebraic models.

4.3.7 Integral formulation of Spring and Slider Models

Ziaming and Katukura (1990) have shown that the elasto-plastic model of equation (4.5a) (which is nothing but the equation of a single spring-slider series combination) can be generalized in integral form to represent a multiple spring-slider model as follows:

$$\dot{M} = \left\{ U(\dot{\phi})U(M)q^+ + U(\dot{\phi})U(-M)f^- + U(-\dot{\phi})U(M)f^+ + U(-\dot{\phi})U(-M)q^- \right\} \dot{\phi} \quad (4.15)$$

where q^+ , f^+ , q^- and f^- are function of M only and are the integral contribution to the total stiffness of the spring-slider pairs in phases 1, 2, 3 and 4 respectively in Fig. 4.4. It can be shown that many of the models discussed earlier can be derived for particular functional representations of q^+ , f^+ , q^- and f^- . Some examples are listed below.

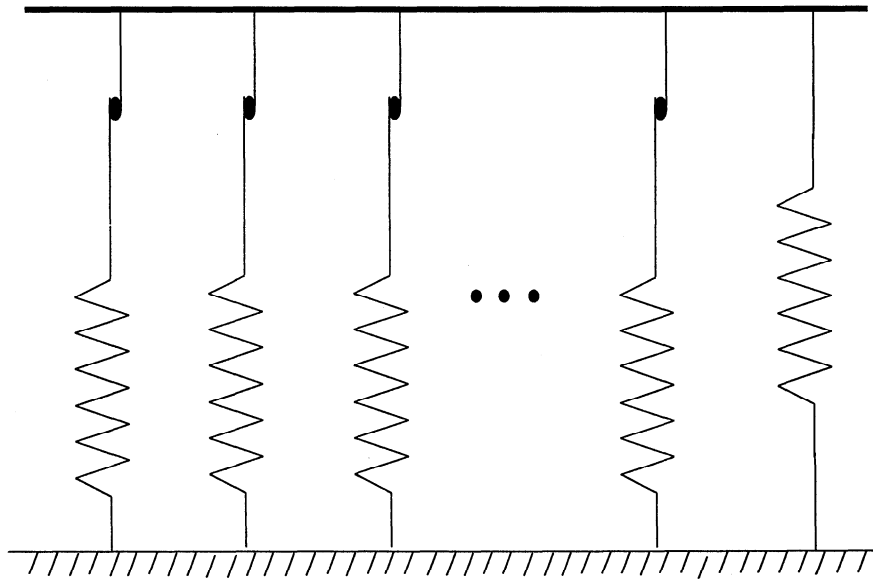


Fig. 4.3 Spring and Slider Model

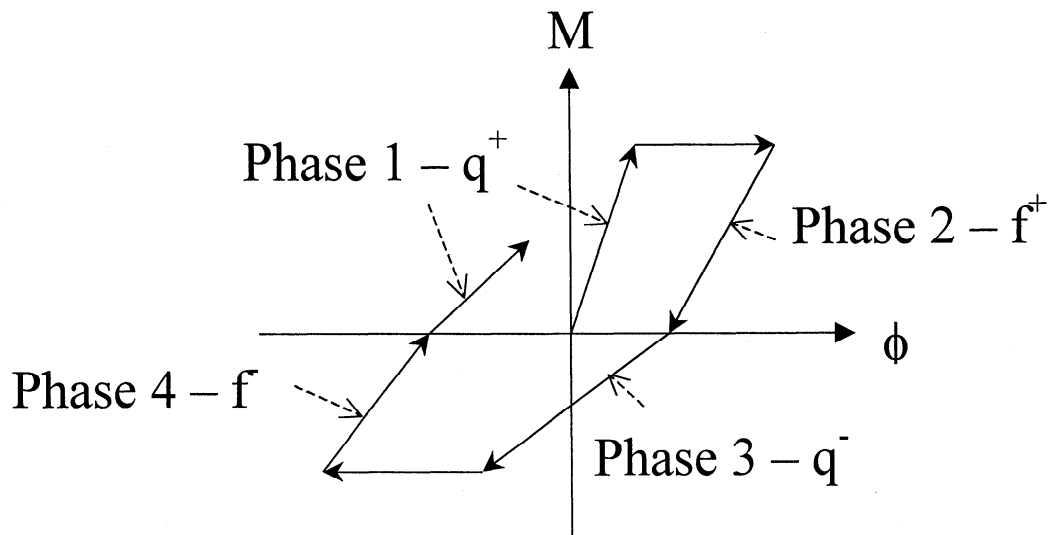


Fig. 4.4 Integral Formulation of Spring and Slider Models

4.3.7.1 Elasto-plastic Model

$$q^+(M) = KU(M_y^+ - M)$$

$$q^-(M) = KU(-M_y^- + M)$$

$$f^+(M) = f^-(M) = K$$

4.3.7.2 Wen-Bouc Model

$$q^+(M) = q^-(M) = K \left[1 - (\eta_1 + \eta_2) \left| \frac{M}{M_y} \right|^N \right]$$

$$f^+(M) = f^-(M) = K \left[1 - (\eta_1 - \eta_2) \left| \frac{M}{M_y} \right|^N \right]$$

4.3.7.3 Vertex-Oriented Polygonal Model without Hardening

$$q^+(M) = KU(M_y^+ - M) \frac{M_y^+ - M}{1 + \phi_{\max}^+ - \phi}$$

$$q^-(M) = KU(-M_y^- + M) \frac{(-M_y^- + M)}{1 - \phi_{\max}^- + \phi}$$

$$f^+(M) = f^-(M) = R_K K$$

where R_K is given by equation (2.1) and ϕ_{\max}^+ and ϕ_{\max}^- are given by equations 3.7 (c) and (d).

4.3.8 Smooth Plasticity Models and Drucker's Stability Postulate

Plasticity models are smoothed for two reasons:

- To represent distributed yielding in macro-constitutive models such as Moment-curvature and Force-deformation relationships
- To alleviate numerical procedures near the yield point.

However, it is found that such smooth models without a yield surface locally violate Drucker's stability postulate which states that, for any load cycle with initial and final load level M_1 , the following inequality must be satisfied:

$$\oint (M - M_1) d\phi \geq 0 \quad (4.16)$$

It can be seen that for a cycle ABC, this is not true. However, for larger cycles like CDE, the postulate holds. Valanis (1981) argues that such local violation of the plasticity postulate does not invalidate the theory and shows that linear viscoelastic and frictional materials violate Drucker's postulate as well. Moreover, since this does not cause any numerical instability and works well for practical load histories, such models can certainly be used for analysis considering their other advantages. The DEM of Iwan (1966) has a piecewise linear transition and does not violate Drucker's postulate. But it involves many more internal variables and does not serve the purpose of easing

numerical solution. Casciati (1989) proposed an additional hysteretic spring with negative energy dissipation, which when added to the Wen-Bouc model reduces the violation of Drucker's postulate.

4.4 Other Strength Degradation Rules

The degradation rules presented in Sections 2 and 3 are examples of a general class of degradation rules based on the theory of internal variables. Other such degradation rules discussed by Ozdemir (1976) and Mostaghel (1999).

4.5 Remarks

The discussion in this section serves to put the hysteretic models developed in sections 2 and 3 in perspective. It shows how the two models fit in the larger picture of one-dimensional inelastic material models. Such an understanding would greatly help in the generalization to three-dimensional inelastic models.

The polygonal model is an abstraction of a combination of a large number of springs and sliders. The smooth model is obtained by smoothening the yield transition in surface-based plasticity models and bears similarity to the endochronic models.

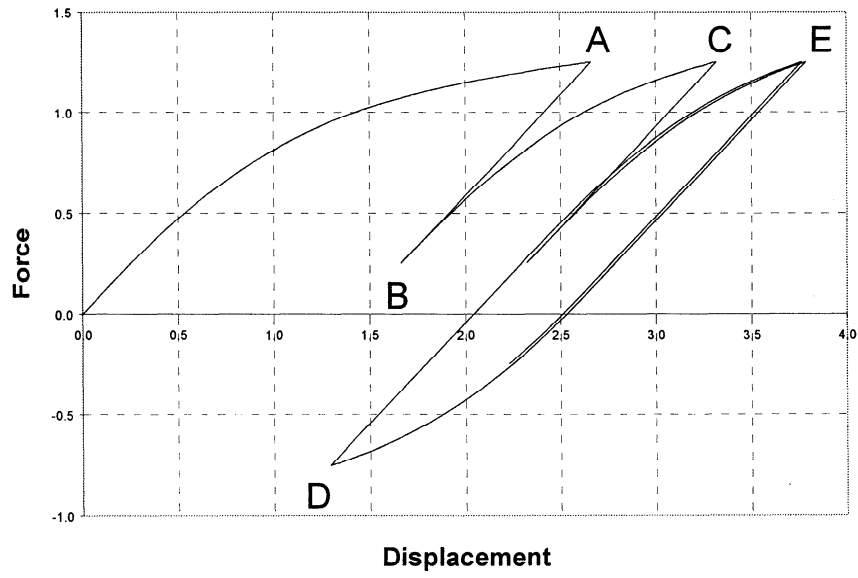


Fig. 4.5 Smooth Model and Drucker's Postulate

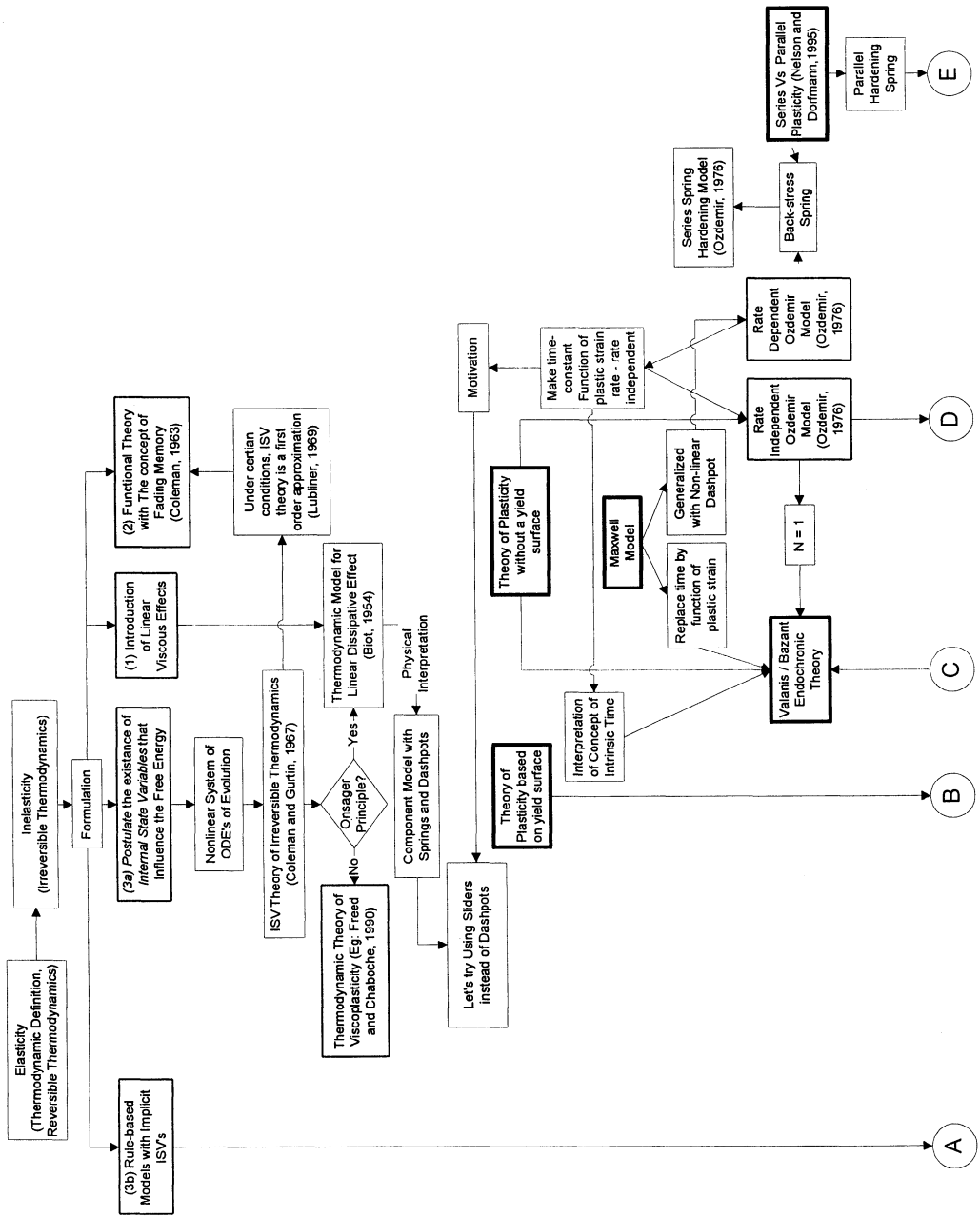


Fig. 4.6 Schematic Diagram of Representation of 1D Inelastic Behavior

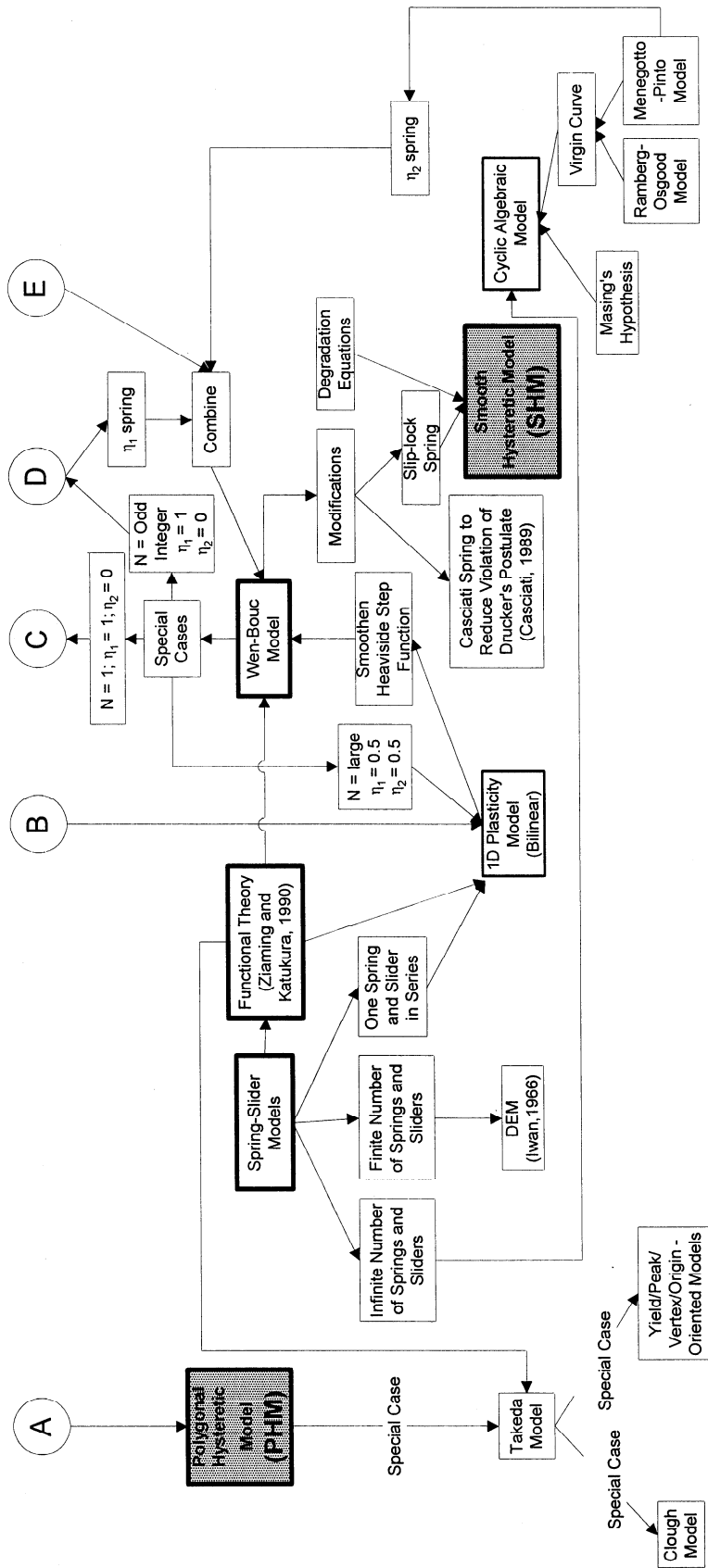


Fig. 4.6 Schematic Diagram of Representation of 1D Inelastic Behavior (contd.)

SECTION 5

IMPLEMENTATION IN COMPUTER PROGRAMS

5.1 Background

The utility of any hysteretic model is realized only when it is implemented in computer platforms for inelastic analysis. The hysteretic models developed in the preceding sections have been incorporated in two computer programs – IDARC2D (Version 5.0) and NSPECTRA. The issues involved in these implementations and some example results are presented in this section.

5.2 IDARC2D Version 5.0

Developed at the University at Buffalo (SUNY), IDARC2D was first introduced in 1987 (Park et al, 1987) for the purpose of analyzing earthquake damage in multistory, reinforced concrete buildings. Since then, numerous enhancements have been added, including the ability to analyze a wide variety of structures, structural materials, and damping devices and analysis after the first onset of damage. New features are continuously being added to IDARC2D and its newest version is Version 5.0. More information about this program can be obtained from its web site, <http://civil.eng.buffalo.edu/idarc2d50>.

5.2.1 Implementation of Hysteretic Model

IDARC solves the equations of equilibrium of the structure incrementally. Since the elements involved are frame elements, that are internally statically determinate, IDARC uses a flexibility-based element formulation and the hysteretic model is used to represent the behavior of the end-section of an element. (Details can be found in Valles et al, 1996). This results in the hysteretic model receiving a moment or force increment from the global system. This would require the hysteretic model to be operated by force control resulting in costly iterations at both the local and global levels. IDARC circumvents this problem by using the method of one-step correction (Park et al, 1987). The process is shown in Fig. 5.1. The model returns the unbalanced moment to the global system. All such unbalanced moments and forces are assemble together and applied to the whole structure as an equivalent external load vector in the next analysis step.

5.2.2 Example

The example presented here is the analysis of a full-scale model of a circular column tested under cyclic loading. Detailed description of this example is provided by Valles et al, 1996. Figure 5.2 shows the test setup and the applied displacement history. Figure 5.3 shows the experimentally obtained force-displacement response and the response predicted by IDARC using the vertex-oriented version of the PHM. An extensive case study using this program is reported by Naeim et al, 1998.

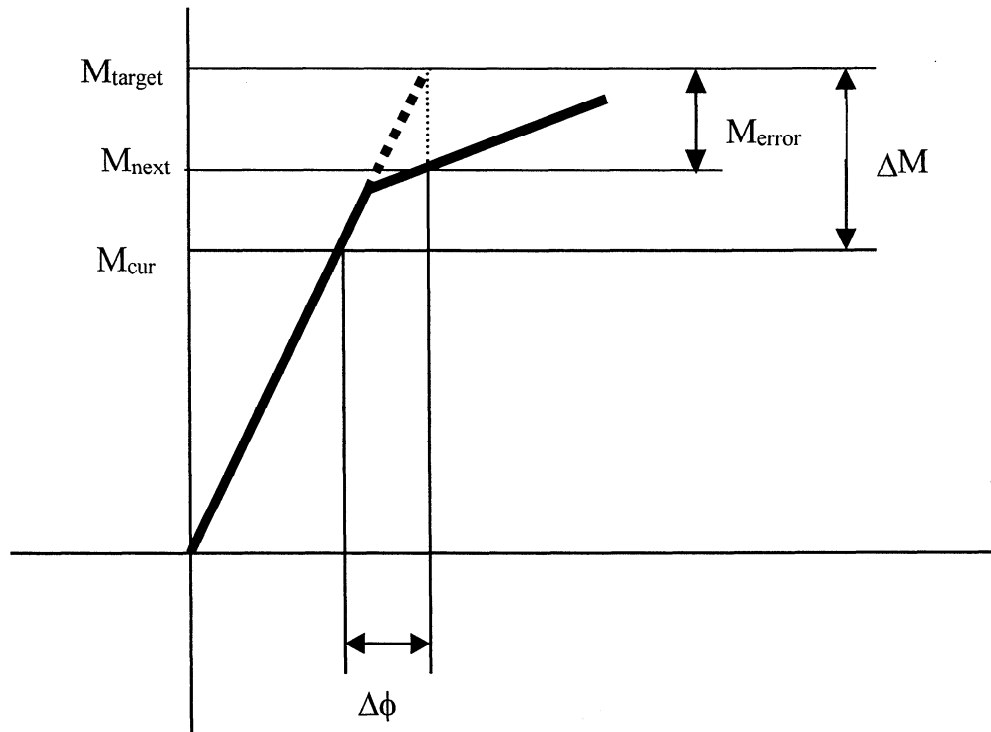


Fig. 5.1 The Method of One-step Correction

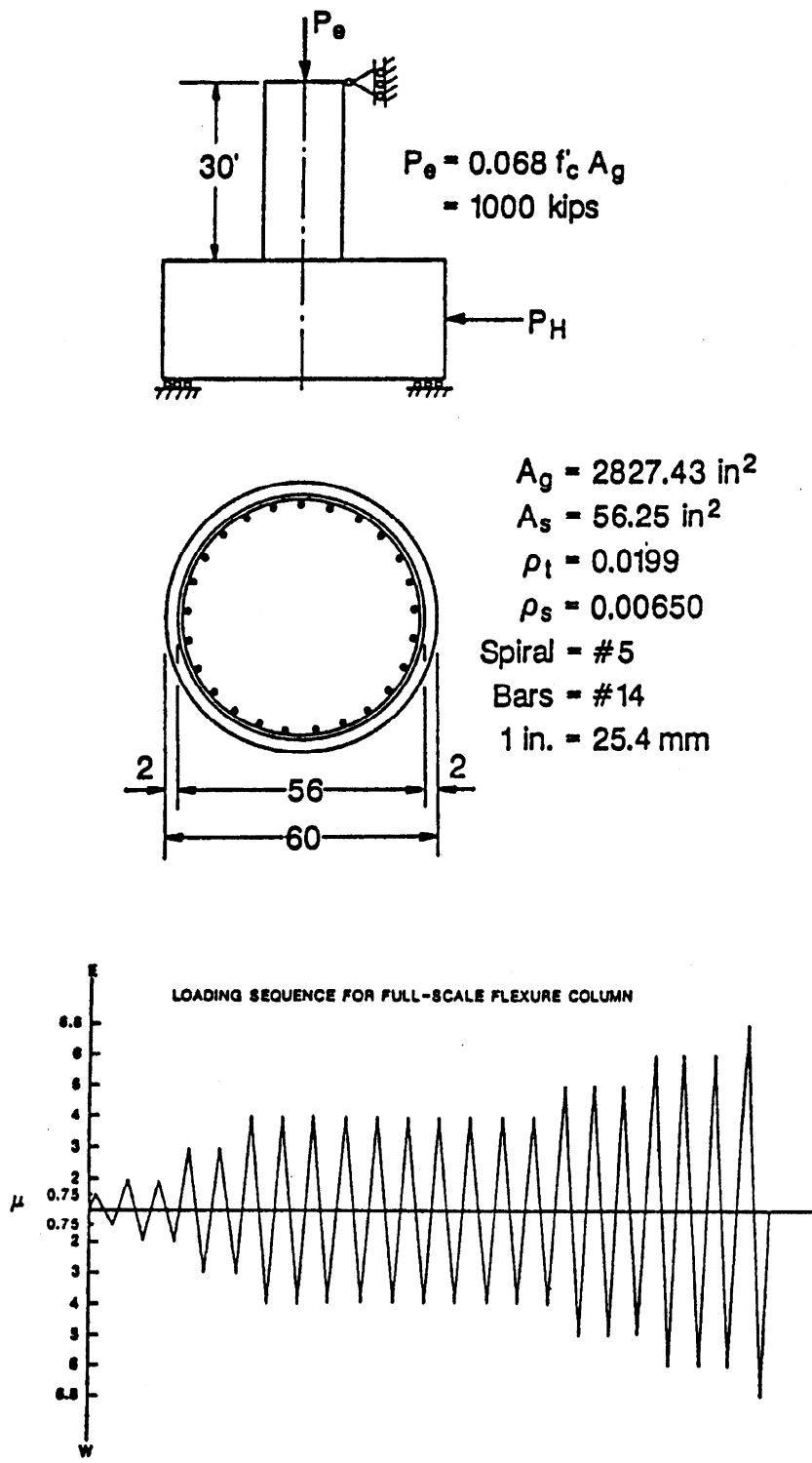
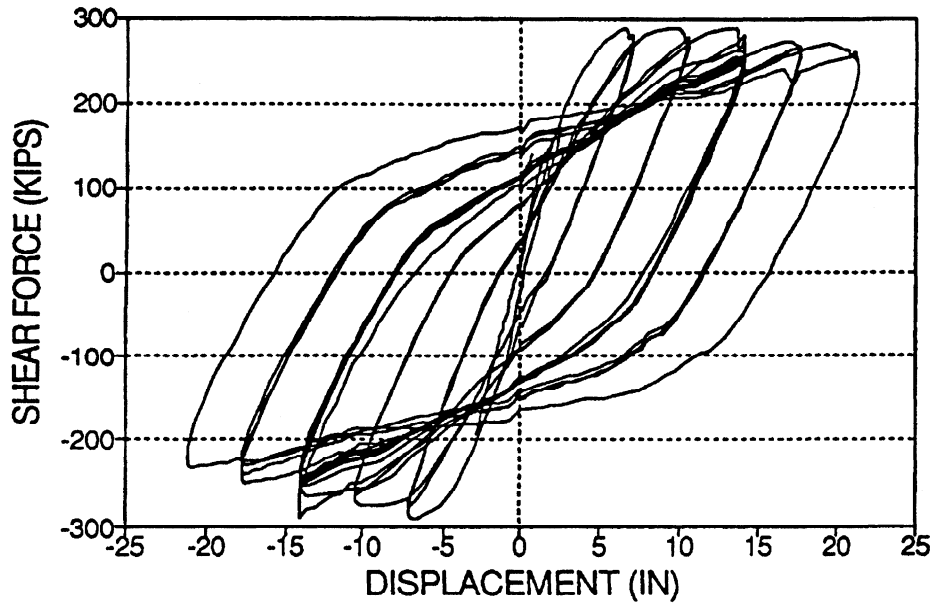
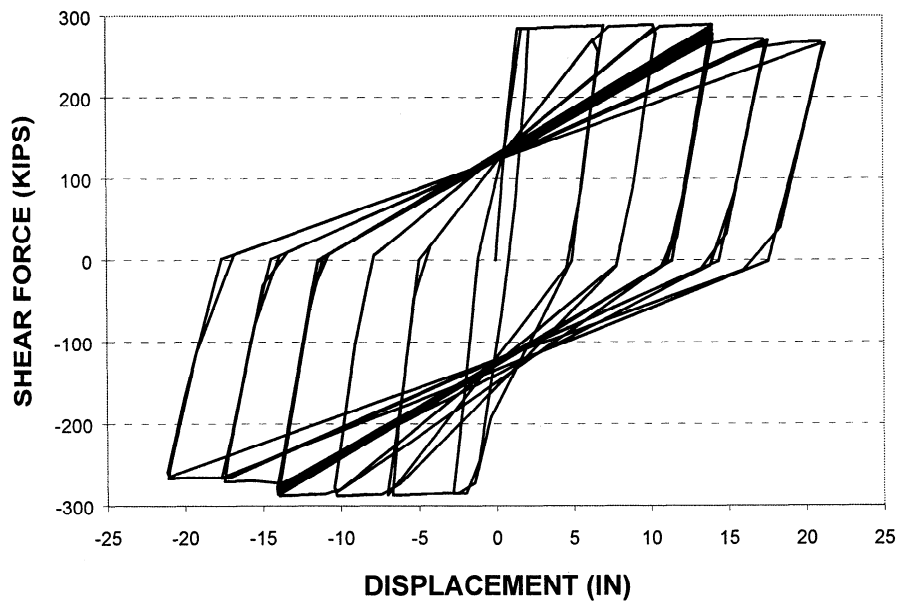


Fig. 5.2 Configuration and Loading of Test Structure for IDARC Example (Valles et al, 1996)



(a) Force-displacement response from experiment (Valles et al, 1996)



(b) Force-displacement response from IDARC simulation
 (Vertex-oriented PHM, $\beta_1 = 0.1$, $\beta_2 = 0.1$, $\mu_{ult} = 3.125$, $\alpha = 9.0$)

Fig. 5.3 Force-displacement Response of IDARC Example

5.3 NSPECTRA

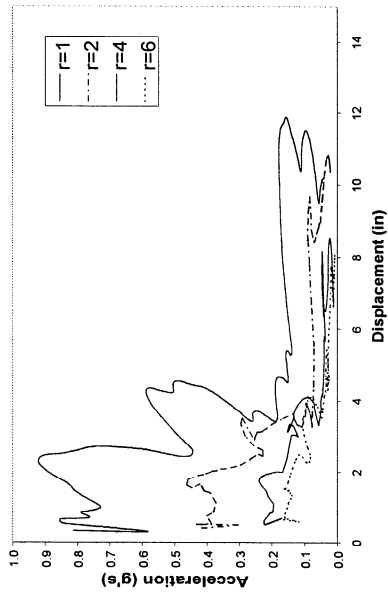
Developed at the University at Buffalo, NSPECTRA is a computer program for obtaining the response spectra of nonlinear systems. The program can perform the analysis for a collection of ground motions (maximum 200 ground motions) returning the response spectra for each ground motion and the average and standard deviation response spectra of the collection. The program can also print out the time history response for a particular pendulum in the spectrum. More information about this program can be obtained from its web site, <http://civil.eng.buffalo.edu/nspectra>.

5.3.1 Implementation of Hysteretic Model

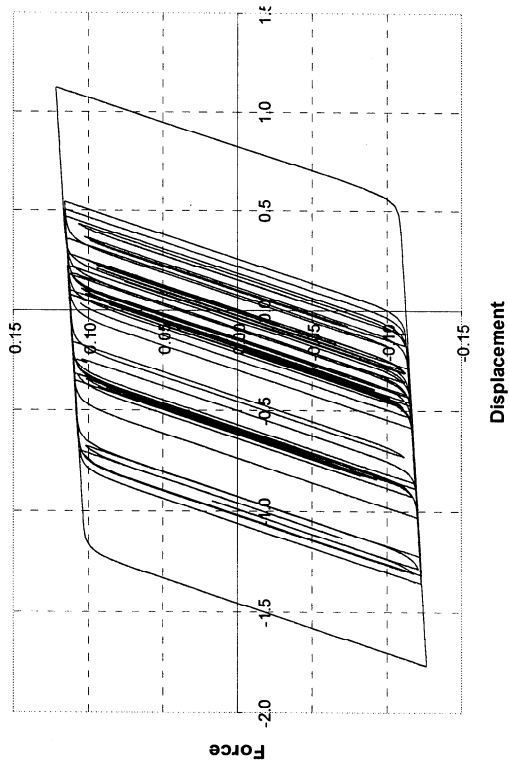
NSPECTRA integrates the equation of motion of a nonlinear SDOF system using the Newmark- β method. It calls the hysteretic model with the current values for force, displacement and other internal variables and the displacement increment. The hysteretic model is thus driven by displacement control. The model in turn returns the force increment (or decrement) and the updated values for the internal variables.

5.3.2 Examples

NSPECTRA is run with the Elcentro ground motion with and without degradation. The results are shown in Fig. 5.4.

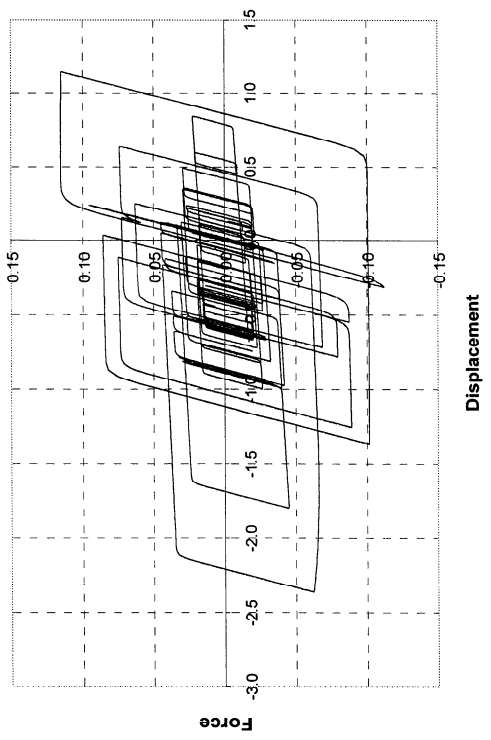


(a) Inelastic composite spectra without degradation

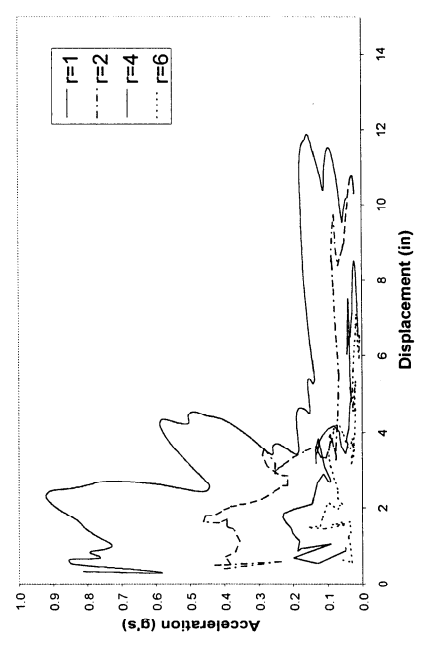


(b) Sample time history of displacement without degradation

Fig. 5.4 Example from NSPECTRA



(d) Sample time history of displacement without degradation



(c) Inelastic composite spectra with degradation
 $(\beta_1 = 0.5, \beta_2 = 0.2, \mu_{ult} = 10)$

Fig. 5.4 Example from NSPECTRA (contd.)

SECTION 6

CONCLUSIONS AND REMARKS

Two hysteretic degrading models –a polygonal and a smooth – have been developed. The development was based on stiffness, rate of stiffness changes and on the adjustments of the yield characteristics. Changing the yielding level and the stiffness of the system, both models accommodate degrading of the hysteretic system. The two parameters can be adjusted in a combination which can simulate strength deterioration, stiffness degradation and pinching (or slip). The polygonal model is more cumbersome in formulation however, it establishes a direct relation between force and displacement (generalized) which permits reversal of control by force or displacement. The smooth model has the advantage that can be solved simultaneously with the equations of motion therefore minimizing the need for iterations. This model can be used in state space approach as indicated by Simeonov et al., 1999.

The hysteretic models and their solutions were developed for the nonlinear analyses of frame structures and these models were implemented in several computer programs such as IDARC2D, NSPECTRA (for development of inelastic spectra), and NONLIN (a derivative of well known program DRAIN2D). The formulations are independent of computer program and can be used as objects in advanced programming.

This report attempts to present a unified theory, which leads to the development of the above models. Starting from the principles of thermodynamics, the developments by prominent researchers are surveyed, and the assumptions and the compromises leading

to newer models were pointed out. Both the polygonal and the smooth models are results of such reductions and developments.

Progressive collapse analysis of structures can utilize these hysteretic models but such analysis tools need to be developed yet. Effective solution algorithms for such potential analysis is the State-Space Approach presented by Simeonov et al, 1999.

SECTION 7

REFERENCES

- Allen, D.H. and Harris, C.E. (1990). "A Review of Nonlinear Constitutive Models for Metals", NASA Technical Memorandum 102727, NASA Langley Research Center, Hampton, Virginia.
- Aoyama, H. (1971). "Analysis of a School Building damaged during the Tockachi-Oki Earthquake", Proceedings of the Kanto District Symposium of AIJ, Tokyo, Japan.
- Atalay, M.B. and Penzien, J. (1975). "The Seismic Behavior of Critical Regions of Reinforced Concrete Components influenced by Moment, Shear and Axial Force"" UCB/EERC Report No. 75-19, University of California, Berkeley.
- Baber, T.T. and Noori, M.N. (1985). "Random Vibration of Degrading Pinching systems", Journal of Engineering Mechanics, Vol. 111, No. 8, pp. 1010-1026.
- Bazant, Z.P. and Bhat, P. (1976). "Endochronic theory of inelasticity and failure of concrete", Journal of Engineering Mechanics, ASCE, 12(4), 701-722.
- Beck, J.L. and Jayakumar, P. (1996). "Class of Masing Models for Plastic Hysteresis in Structures", Building an International Community of Structural Engineers Vol. 2, Proceedings of Structures Congress XIV, ASCE, Chicago, Illinois.
- Biot, M.A. (1954). "Theory of Stress-Strain Relations in Anisotropic Viscoelasticity and Relaxation Phenomena", Journal of Applied Physics, Vol. 25, No. 11, pp. 1385-1391.
- Bodner, S.R. (1968). Mechanical Behavior of Materials under Dynamic Loads, Springer-Verlag, New York.
- Bodner, S.R. and Partom, Y. (1975). "Constitutive equations for elastic-viscoplastic strain-hardening materials" *J. Appl. Mech.*, 62, 385-389.
- Bouc, R. (1967). "Forced vibration of mechanical systems with hysteresis", Proceedings of the 4th Conference on Non-linear Oscillations, Prague.
- Bruneau, M., Uang, C. and Whittaker, A. (1998) Ductile Design of Steel Structures, McGraw-Hill, New York.
- Capecchi, D. (1991). "Periodic response and stability of hysteretic oscillators", Dynamics and Stability of Systems, Oxford University Press, Vol. 6, No. 2, pp. 89-106.
- Casciati, F. (1989). "Stochastic Dynamics of Hysteretic Media", Structural Safety, Vol. 6, pp. 259-269.

- Caspe, M.S., and Reinhorn, A.M. (1986), "The Earthquake Barrier - A Solution for Adding Ductility to Otherwise Brittle Buildings", Base Isolation and Passive Energy Dissipation, C. Rojahn (Ed.), Applied Technology Council, ATC-17, pp.331-362.
- Chiang, D Y. and Beck, J L. (1994). "New class of distributed-element models for cyclic plasticity - II. On important properties of material behavior", International Journal of Solids & Structures. Vol. 31, No. 4, pp. 485-496.
- Chiang, D Y. and Beck, J L. (1994). "New class of distributed-element models for cyclic plasticity - I. Theory and application", International Journal of Solids & Structures. Vol. 31, No. 4, pp. 469-484.
- Clough, R.W. (1966). "Effect of Stiffness Degradation on Earthquake Ductility Requirement", Report No. 6614, Structural and Material Research, University of California, Berkeley.
- Coleman, B.D. (1964). "Thermodynamics of Materials with Memory", Archive for Rational Mechanics and Analysis", Vol.17, No. 1, 1-46.
- Coleman, B.D. and Gurtin, M.E. (1967). "Thermodynamics with Internal State Variables", Journal of Chemical Physics, Vol. 47, No. 2, pp. 597-613.
- Constantinou, M.C. and Adnane, M.A. (1987). "Dynamics of Soil-Base-Isolated-Structure Systems", Report to the National Science Foundation.
- Freed, A D., Chaboche, J L. and Walker, K P. (1991). "Viscoplastic theory with thermodynamic considerations", Acta Mechanica, Vol. 90, No. 1, pp. 155-174.
- Fritzen, P. and Wittekindt, J. (1997). "Numerical Solution of viscoplastic constitutive equations with internal state variables Part I: Algorithms and implementation", Mathematical Methods in Applied Sciences, Vol. 30, pp. 1411-1425.
- Fukada, Y. (1969). "A Study on the Restoring Force Characteristics of Reinforced Concrete Buildings", Proceedings of the Kanto District Symposium of AIJ, Tokyo, Japan.
- Fung, Y.C. (1965). Foundations of Solid Mechanics, Prentice-Hall, Inc., New Jersey.
- Gomes, A. and Appleton, J. (1997). "Nonlinear cyclic stress-strain relationship of reinforcing bars including buckling", Engineering Structures, Vol. 19, No. 10, pp. 822-826.
- Graesser, E.J. and Cozzarelli, F.A. (1991), " A multidimensional hysteretic model for plastically deforming metals in energy absorbing devices", Technical Report NCEER-91-0006, National Center for Earthquake Engineering Research, State University of New York at Buffalo.

- Iwan, W.D. (1966). "A distributed-element model for hysteresis and its steady-state dynamic response" *Journal of Applied Mechanics*, Vol. 33, No. 42, pp. 893-900.
- Jayakumar, P. (1987). "Modeling and Identification in Structural Dynamics", Report No. EERL 87-01, Earthquake Engineering Research Laboratory, California Institute of Technology, Pasadena, California.
- Komkov, V. and Valanis, K. (1981). "On the Properties of Materials and the Concepts of Time and Space", *Speculations in Science and Technology*, Vol. 4, No. 2, pp. 157-173.
- Kustu, O. and Boukamp, J.G. (1975). "Behavior of Reinforced Concrete Deep Beam-Column Subassemblages under Cyclic Loads", UCB/EERC Report No. 73-8, University of California, Berkeley.
- Lubliner, J. (1969). "On Fading Memory in Materials of Evolutionary Type", *Acta Mechanica*, Vol. 8, No. 1-2, pp. 75-81.
- Lubliner, J. (1990). *Plasticity Theory*, Macmillan, New York.
- Madan, A., Reinhorn, A.M., Mander, J. and Valles, R. (1997). "Modeling of Masonry Infill Panels for Structural Analysis", *Journal of Structural Engineering*, Vol. 123, No. 10, pp. 1295-1302.
- Malvern, L.E. (1969). *Introduction to the Mechanics of a Continuous Medium*, Prentice-Hall Inc., New Jersey.
- Mazzolani, F.M. and Piluso, V. (1996). *Theory and Design of Seismic Resistant Steel Frames*, Chapman & Hall, New York.
- Moran, M.J. and Shapiro, H. (1995). *Fundamentals of Engineering Thermodynamics*, John Wiley & Sons, New York.
- Mostaghel, N. (1999). "Analytical Description of Pinching, Degrading Hysteretic Systems", *Journal of Engineering Mechanics*, Vol. 125, No. 2, pp. 216-224.
- Muto, K., Hisada, T., Tsugawa, T. and Bessho, S. (1973). "Earthquake Resistant Design of a 20-story Reinforced Concrete Building", *Proceedings of the 5th WCEE*, Rome.
- Naeim, F., Skliros, K., Reinhorn, A. M., Sivaselvan, M. V., (1998). "Effects of Hysteretic Deterioration Characteristics on Seismic Response of Moment Resisting Steel Structures", JAMA Report, John A. Martin & Associates, Inc., Los Angeles.
- Nagarajaiah, S., Reinhorn, A.M. and Constantinou, M.C. (1989). "Nonlinear Dynamic Analysis of Three Dimensional Base Isolated Structures (3D-BASIS)", Technical Report NCEER-89-0019, State University of New York at Buffalo.

- Nakata, S., Sproul, T. and Penzien, J. (1978). "Mathematical Modeling of Hysteresis Loops for Reinforced Concrete Columns", UCB/EERC Report No. 78-11, University of California, Berkeley.
- Nelson, R.B. and Dorfmann, A. (1995). "Parallel elastoplastic models of inelastic material behavior", *Journal of Structural Engineering*, ASCE, Vol. 121, No. 10, pp. 1089-1097.
- Ozdemir, H. (1976). "Nonlinear transient dynamic analysis of yielding structures", Ph.D. dissertation, University of California, Berkeley.
- Park, Y.J., Reinhorn, A.M. and Kunnath, S.K. (1987). "IDARC: Inelastic Damage Analysis of Reinforced Concrete Frame – Shear-wall Structures", Technical Report NCEER-87-0008, State University of New York at Buffalo.
- Press, W.H., Teukolsky, S.A., Vetterling, W.T. and Flannery, B.P. (1992). *Numerical Recipes in Fortran*, Cambridge University Press, New York.
- Priestley, M.J. and Calvi, G.M. (1996). *Seismic Design and Retrofit of Bridges*, John Wiley & Sons, New York.
- Ramberg, W. and Osgood, W.R. (1943). "Description of Stress-Strain Curves by Three Parameters", Technical Note 902, National Advisory Committee on Aeronautics.
- Reichman, Y. and Reinhorn, A.M. (1995). "Extending Seismic Life Span of Bridges", *Structural Engineering Review – Progress in Bridge Engineering*, Pergamon Press, Vol. 7, No. 3, pp. 207-218.
- Reinhorn, A.M., Madan, A., Valles, R.E. Reichmann, Y. and Mander, J.B. (1995). "Modeling of Masonry Infill Panels for Structural Analysis", Technical Report NCEER-95-0018, State University of New York at Buffalo.
- Ristinmaa, M. (1999). "Thermodynamic Formulation of Plastic Work Hardening Materials", *Journal of Engineering Mechanics*, Vol. 125, No. 2, pp. 152-155.
- SAC Joint Venture (1996). "Experimental Investigations of Beam-Column Subassemblages" Report No. SAC-96-01, Parts I and II, SAC Joint Venture, Sacramento, California.
- Shi, P. and Babuska, I. (1997). "Analysis and computation of a cyclic plasticity model by the aid of DDASSL" *Computational Mechanics*, Vol. 19, No. 4, pp. 380-385.
- Simeonov, V., Sivaselvan, M.V. and Reinhorn, A.M. (1999), "Nonlinear Analysis of Structural Frame Systems by the State-Space Approach", *Proceedings of the European Conference on Computational Mechanics*, Munich, Germany, September, 1999. (To appear)

- Soong, T.T. and Dargush, G.F. (1997). *Passive Energy Dissipation Systems in Structural Engineering*, John Wiley & Sons, New York.
- Takayanagi, T. and Schnobrich, W.C. (1977). "Computed Behavior of Coupled Shear Walls", *Proceedings of the 6th WCEE*, New Delhi.
- Takeda, T., Sozen, M.A. and Nielsen, N.N. (1970). "Reinforced Concrete Response to Simulated Earthquakes", *Journal of Structural Division, ASCE*, Vol. 96, No. ST-12, pp. 2557-2573.
- Tani, S. and Nomura, S. (1973). "Response of Reinforced Concrete Structures Characterized by Skeleton Curve and Normalized Characteristic Loops to Ground Motion", *Proceedings of the 5th WCEE*, Rome.
- Thyagarajan, R.S. (1989). "Modeling and Analysis of Hysteretic Structural Behavior", Report No. EERL 89-03, California Institute of Technology, Pasadena, California.
- Valanis, K.C. (1971). "A theory of viscoplasticity without a yield surface", *Archives of Mechanics*, Vol. 23, No. 4, pp. 517-533.
- Valanis, K.C. (1980). "Fundamental Consequences of a New Intrinsic Time Measure – Plasticity as a Limit of the Endochronic Theory", *Archives of Mechanics*, Vol. 32, No. 2, pp. 171-191.
- Valles, R. E., Reinhorn, A.M., and Barrón, R. (1999), "Seismic Evaluation of a Low-Rise RC Building in the Vicinity of the New Madrid Seismic Zone," Technical Report MCEER-99-xxxx, National Center for Earthquake Engineering Research, State University of New York at Buffalo (in press).
- Valles, R. E., Reinhorn, A.M., Kunnath, S.K., Li, C. and Madan, A. (1996), "IDARC 2D 2D Version 4.0: A Program for the Inelastic Damage Analysis of Buildings", Technical Report NCEER-96-0010, National Center for Earthquake Engineering Research, State University of New York at Buffalo.
- Wen, Y.K. (1976). "Method of Random Vibration of Hysteretic Systems", *Journal of the Engineering Mechanics Division, ASCE*, Vol. 102, No. EM2, pp. 249-263.
- Ziaming, L. and Katukura, H. (1990). "Markovian Hysteretic Characteristics of Structures", *Journal of Engineering Mechanics*, Vol. 116, No. 8, pp. 1798-1811.

APPENDIX A

IMPLEMENTATION DETAILS OF THE POLYGONAL HYSTERETIC MODEL

Table A.1 Subroutines and their functions

SUBROUTINE	FUNCTION
HYSCONTROL	Main Hysteretic Model Control Subroutine. (Fig. 2.8)
CONTROL1	This subroutine changes to a Load-reversal branch when there is a change in the direction of loading. (Fig. 2.9)
CONTROL2	If the target point does not lie on the current branch, this subroutine keeps switching branches till target-point lies on current branch, each time setting the current point to the end point of the current branch and updating the hysteretic energy each time. (Fig. 2.10)
CONTROL3	When this subroutine is called, the target point always lies on the current branch. The target point is found by interpolating between the end points of the current branch. It also degrades the strength, causing a drop in the backbone curve. (Fig. 2.11)
POINTS	Computes the coordinates of any of the control points, given the database variables.
NEXT_BRANCH	Uses the branch-transition rules to determine the number of the next branch, given the load increment and the database variables.

Table A.2 Variables Governing PHM

SYMBOL	MEANING
M_{cur}	Current Moment level in the section
ϕ_{cur}	Current Curvature of the section
ΔM	Moment Increment
EI	Slope of the current branch
M_{max}^+	Maximum positive moment reach by the section at any time
ϕ_{max}^+	Maximum positive curvature reached by the section at any time
M_{max}^-	Maximum negative moment reach by the section at any time
ϕ_{max}^-	Maximum negative curvature reached by the section at any time
M_y^+	Current (degraded) value of positive yield moment
M_y^-	Current (degraded) value of negative yield moment
M_{vertex}^+	Moment at the current vertex point on the positive side.
ϕ_{vertex}^+	Curvature at the current vertex point on the positive side.
M_{vertex}^-	Moment at the current vertex point on the negative side.
ϕ_{vertex}^-	Curvature at the current vertex point on the negative side.
M_{cr}^+	Positive Cracking Moment
M_{cr}^-	Negative Cracking Moment
K_0	Initial Elastic slope

(Boxed variables are Backbone Parameters. Others are *database* or *internal* variables)

Table A.2 Variables Governing PHM (contd.)

SYMBOL	MEANING
M_{y0}^+	Initial Positive Yielding Moment
ϕ_{y0}^+	Initial Positive Yield curvature
M_{y0}^-	Initial Negative Yielding Moment
ϕ_{y0}^-	Initial Negative Yield curvature
ϕ_u^+	Ultimate Positive Curvature
ϕ_u^-	Ultimate Negative Curvature
a^+	Positive Post-yield slope as a fraction of the initial elastic slope
a^-	Negative Post-yield slope as a fraction of the initial elastic slope
α	Stiffness Degradation Parameter
β	Strength Degradation Parameter
γ	Slip (or pinching) Parameter.

(Boxed variables are Backbone Parameters. Others are *database* or *internal* variables)

Table A.3 Point Formulas

POINT	FORMULA		
	ϕ	M	Other Terms Used
1	M_{cr}^+ / K_0	M_{cr}^+	-
2	M_{cr}^- / K_0	M_{cr}^-	-
3	ϕ_{y0}^+	M_y^+	-
4	ϕ_{y0}^-	M_y^-	-
5	ϕ_{max}^+	M_{max}^+	-
6	ϕ_{max}^-	M_{max}^-	-
7	ϕ_u^+	$M_y^+ + K_{sh}^+(\phi_u^+ - \phi_{y0}^+)$	$K_{sh}^+ = a^+ K_0$
8	ϕ_u^-	$M_y^- + K_{sh}^-(\phi_u^- - \phi_{y0}^-)$	$K_{sh}^- = a^- K_0$
9	9'	Point of intersection of : <ul style="list-style-type: none"> • Line joining point 4 and point 8 • Line passing through point $(M_{vertex}^+, \phi_{vertex}^+)$ and having slope $R_K^+ K_0$ 	$R_K^+ = \frac{M_{vertex}^+ + \alpha M_y^+}{K_0 \phi_{vertex}^+ + \alpha M_y^+}$
	9	$\phi_{vertex}^+ - \frac{M_{vertex}^+}{R_K^+ K_0}$	
10	10'	Point of intersection of : <ul style="list-style-type: none"> • Line joining point 3 and point 7 • Line passing through point $(M_{vertex}^-, \phi_{vertex}^-)$ and having slope $R_K^- K_0$ 	$R_K^- = \frac{M_{vertex}^- + \alpha M_y^-}{K_0 \phi_{vertex}^- + \alpha M_y^-}$
	10	$\phi_{vertex}^- - \frac{M_{vertex}^-}{R_K^- K_0}$	

Table A.3 Point Formulas (contd.)

POINT		FORMULA		
		ϕ	M	Other Terms Used
11		Point of intersection of: <ul style="list-style-type: none"> Line joining point 9 and point 13 Branch 1 		-
12		Point of intersection of: <ul style="list-style-type: none"> Line joining point 10 and point 14 Branch 1 		-
13		$WF\phi_{\gamma y}^- + (1-WF)\phi_{\gamma u}^-$	γM_y^-	$R_{K,\max}^+ = \frac{M_{\max}^+ + \alpha M_y^+}{K_0 \phi_{\max}^+ + \alpha M_y^+}$ $\phi_{\gamma u}^- = \phi_{\max}^- - \frac{M_{\max}^- - \gamma M_y^-}{R_{K,\max}^- K_0}$
		If $M_{\max}^- > M_y^-$ and $M < M_{cr}^-$ then		
		M_{cr}^- / K_0	M_{cr}^-	$\phi_y^- = M_y^- / K_0$ $\phi_{\gamma y}^- = \gamma \phi_y^-$ Weighting Factor, $WF = \gamma$
	13'	Point of intersection of: <ul style="list-style-type: none"> Line joining point 8 and point 4 Branch 1 		-
13''		If $\phi_{\text{vertex}}^- > M_y^- / K_0$ then same as Point 2		-
		Else Point of intersection of: <ul style="list-style-type: none"> Line joining point 9 and $(\phi_{\text{vertex}}^-, M_{\text{vertex}}^-)$ Branch 1 		-

Table A.3 Point Formulas (contd.)

POINT		FORMULA		
		ϕ	M	Other Terms Used
14	14	$WF\phi_{\gamma y}^+ + (1-WF)\phi_{\gamma u}^+$	γM_y^+	$R_{K,\max}^- = \frac{M_{\max}^- + \alpha M_y^-}{K_0\phi_{\max}^- + \alpha M_y^-}$
		If $M_{\max}^+ < M_y^+$ and $M > M_{cr}^+$ then		$\phi_{\gamma u}^+ = \phi_{\max}^+ - \frac{M_{\max}^+ - \gamma M_y^+}{R_{K,\max}^+ K_0}$
		M_{cr}^+ / K_0	M_{cr}^+	$\phi_y^+ = M_y^+ / K_0$
	14'	Point of intersection of: <ul style="list-style-type: none"> Line joining point 7 and point 3 Branch 1 		-
14''	14'''	If $\phi_{\text{vertex}}^+ < M_y^+ / K_0$ then same as Point 1		-
		Else Point of intersection of: <ul style="list-style-type: none"> Line joining point 10 and $(\phi_{\text{vertex}}^P, M_{\text{vertex}}^+)$ Branch 1 		-
15		ϕ_{\max}^+	M_{\max}^+	-
16		ϕ_{\max}^-	M_{\max}^-	-

Table A.3 Point Formulas (contd.)

POINT		FORMULA		
		ϕ	M	Other Terms Used
17	A	Point of intersection of: <ul style="list-style-type: none"> • Line joining point 1 and point 3 • Line passing through current point and having slope $R_K^+ K_0$ 		$R_K^+ = \frac{M_{cur} + \alpha M_y^+}{K_0 \phi_{cur} + \alpha M_y^+}$
	B	Point of intersection of: <ul style="list-style-type: none"> • Line joining point 3 and point 5 • Line passing through current point and having slope $R_K^+ K_0$ 		
	C	Point of intersection of: <ul style="list-style-type: none"> • Line joining point 10 and point 14 • Line passing through current point and having slope $R_K^+ K_0$ 		
	D	Point of intersection of: <ul style="list-style-type: none"> • Line joining point 14 and point 15 • Line passing through current point and having slope $R_K^+ K_0$ 		

Table A.3 Point Formulas (contd.)

POINT		FORMULA		
		ϕ	M	Other Terms Used
18	A	Point of intersection of: <ul style="list-style-type: none"> • Line joining point 2 and point 4 • Line passing through current point and having slope $R_K^- K_0$ 		$R_K^- = \frac{M_{cur} + \alpha M_y^-}{K_0 \phi_{cur} + \alpha M_y^-}$
	B	Point of intersection of: <ul style="list-style-type: none"> • Line joining point 4 and point 6 • Line passing through current point and having slope $R_K^- K_0$ 		
	C	Point of intersection of: <ul style="list-style-type: none"> • Line joining point 9 and point 13 • Line passing through current point and having slope $R_K^- K_0$ 		
	D	Point of intersection of: <ul style="list-style-type: none"> • Line joining point 9 and point 13 • Line passing through current point and having slope $R_K^- K_0$ 		

Table A.3 Point Formulas (contd.)

POINT	FORMULA		
	ϕ	M	Other Terms Used
19	Point of intersection of: <ul style="list-style-type: none"> • Line joining point 14 and point 15 • Line passing through current point and having slope $R_K^+ K_0$ 		$R_K^+ = \frac{M_{cur} + \alpha M_y^+}{K_0 \phi_{cur} + \alpha M_y^+}$
20	Point of intersection of: <ul style="list-style-type: none"> • Line joining point 10 and point 14 • Line passing through current point and having slope $R_K^- K_0$ 		$R_K^- = \frac{M_{cur} + \alpha M_y^-}{K_0 \phi_{cur} + \alpha M_y^-}$
21	$\phi_{current}$	$M_{current}$	-

Table A.4 Map of Branch Connectivity

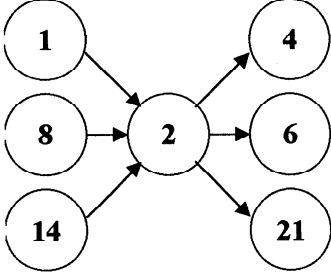
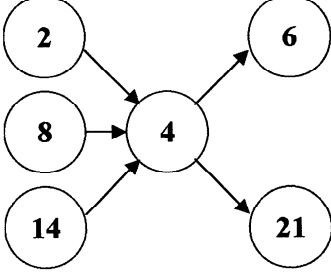
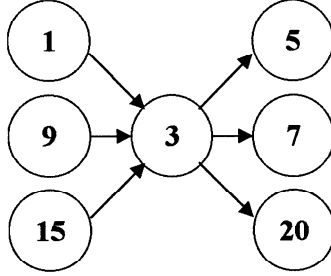
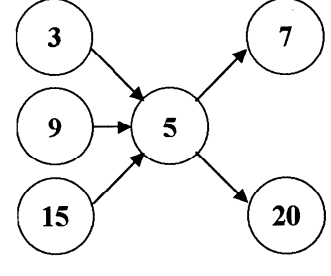
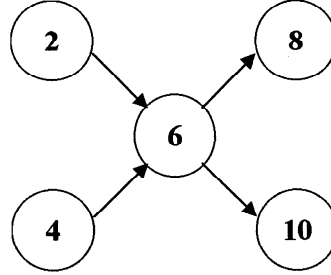
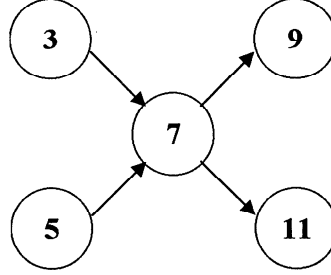
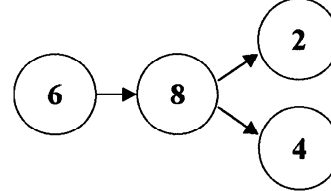
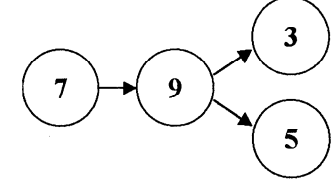
Branch 2	Branch 4
 <pre> graph LR 1((1)) --> 2((2)) 8((8)) --> 2 14((14)) --> 2 2 --> 4((4)) 2 --> 6((6)) 2 --> 21((21)) </pre>	 <pre> graph LR 2((2)) --> 4((4)) 8((8)) --> 4 14((14)) --> 4 4 --> 6((6)) 4 --> 21((21)) </pre>
Branch 3	Branch 5
 <pre> graph LR 1((1)) --> 3((3)) 9((9)) --> 3 15((15)) --> 3 3 --> 5((5)) 3 --> 7((7)) 3 --> 20((20)) </pre>	 <pre> graph LR 3((3)) --> 5((5)) 9((9)) --> 5 15((15)) --> 5 5 --> 7((7)) 5 --> 20((20)) </pre>
Branch 6	Branch 7
 <pre> graph LR 2((2)) --> 6((6)) 4((4)) --> 6 6 --> 8((8)) 6 --> 10((10)) </pre>	 <pre> graph LR 3((3)) --> 7((7)) 5((5)) --> 7 7 --> 9((9)) 7 --> 11((11)) </pre>
Branch 8	Branch 9
 <pre> graph LR 6((6)) --> 8((8)) 8 --> 2((2)) 8 --> 4((4)) </pre>	 <pre> graph LR 7((7)) --> 9((9)) 9 --> 3((3)) 9 --> 5((5)) </pre>

Table A.4 Map of Branch Connectivity (contd.)

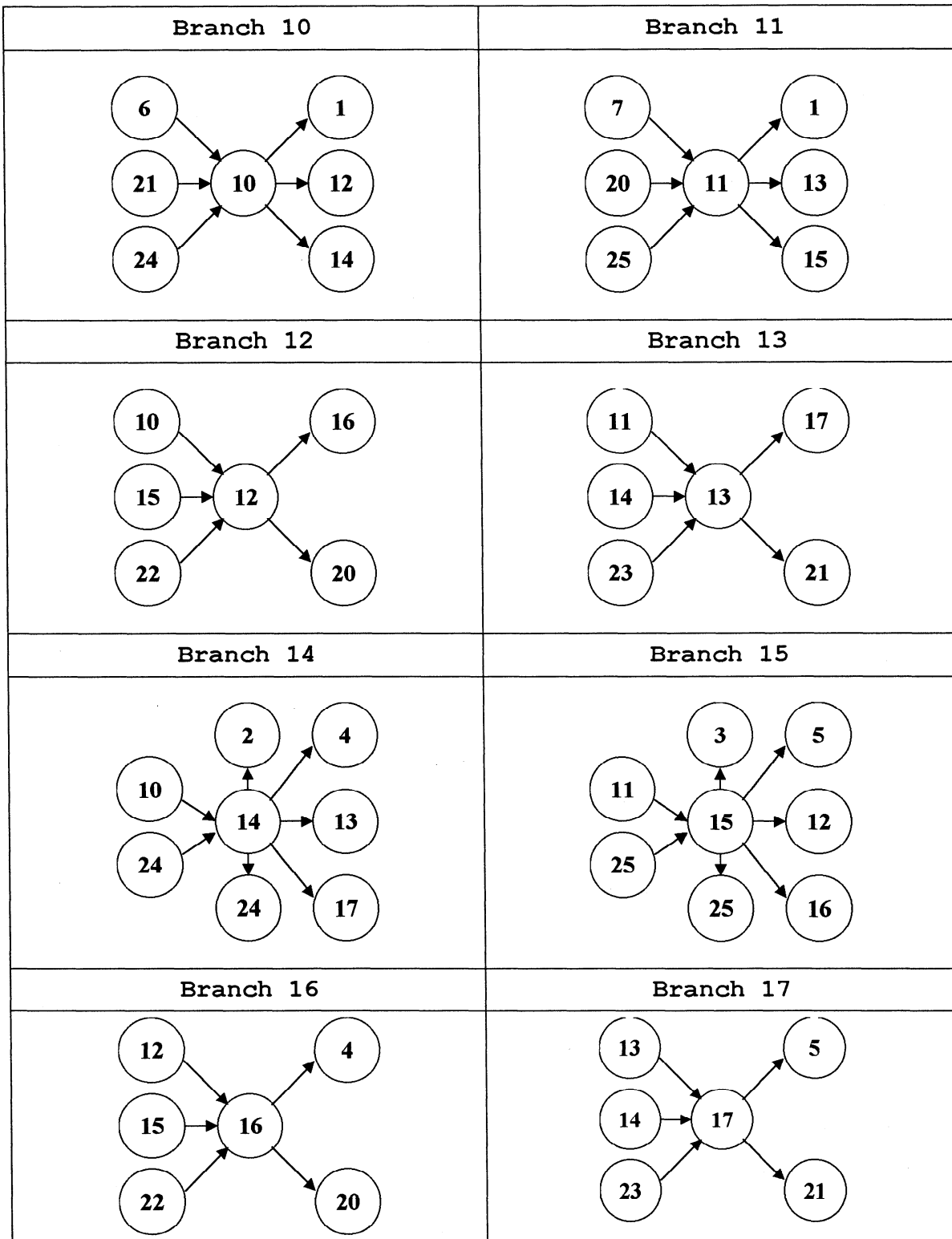


Table A.4 Map of Branch Connectivity (contd.)

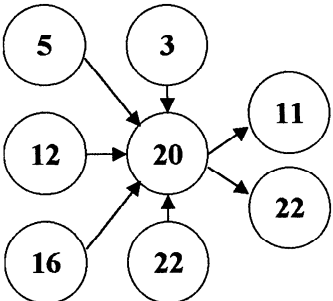
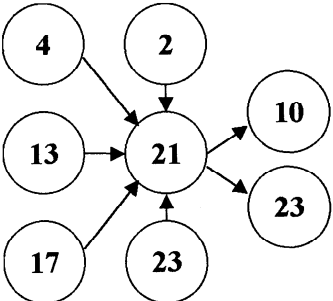
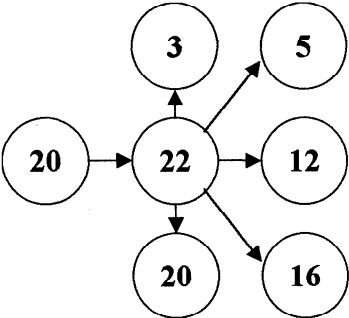
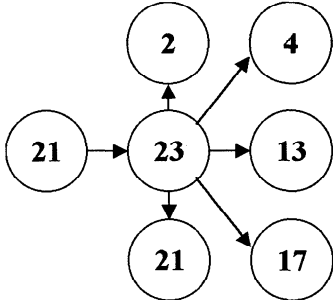
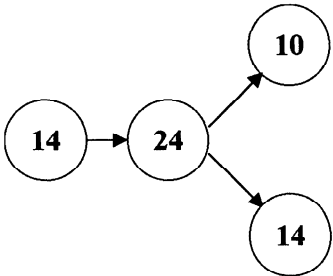
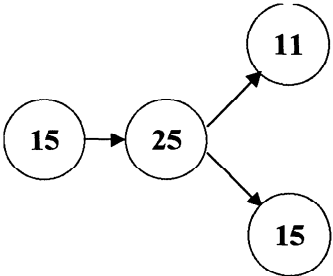
Branch 20	Branch 21
	
Branch 22	Branch 23
	
Branch 24	Branch 25
	

Table A.5 Starting and ending points of branches

Branch	1	2	3	4	5	6	7	8	9	10	11	12	13	14	15	16	17	18	19	20	21	22	23	24	25
Start Pt	1	1	2	3	4	5	6	9	10	9	10	11	12	21	21	13	14	14	21	21	21	21	21	21	21
End Pt	2	3	4	7	8	9	10	5	6	11	12	13	14	17	18	16	15	15	10	10	9	18	17	19	20

Table A.6 Rules for Change of Branch

Current Branch	Next Branch	Condition	
		Force Control	Displacement Control
1	1	In this case, $(\phi_{start}^1, M_{start}^1)$ is always on the negative end of Branch 1 and $(\phi_{end}^1, M_{end}^1)$ is always on the positive side. $M_{start}^1 < M_{cur} + \Delta M < M_{end}^1$	$\Delta\phi (\phi_{end}^1 - \phi_{start}^1) < 0$, i.e., there is a load reversal. Also swap Start and Endpoints of Branch 1 in this case
	2	Not on Branch 1 and $\Delta M > 0$	$\Delta\phi (\phi_{end}^1 - \phi_{start}^1) > 0$ $\Delta\phi > 0$
	3	Not on Branch 1 and $\Delta M < 0$	$\Delta\phi (\phi_{end}^1 - \phi_{start}^1) > 0$ $\Delta\phi < 0$
2	4	$\Delta M > 0$	$\Delta\phi > 0$
	6	$\Delta M < 0, M_{cur} > M_{max}^+$	$\Delta\phi < 0, M_{cur} > M_{max}^+$
	21	$\Delta M < 0, M_{cur} < M_{max}^+$ (See Fig. A.1)	$\Delta\phi < 0, M_{cur} < M_{max}^+$ (See Fig. A.1)
3	5	$\Delta M < 0$	$\Delta\phi < 0$
	7	$\Delta M > 0, M_{cur} < M_{max}^-$	$\Delta\phi > 0, M_{cur} < M_{max}^-$
	20	$\Delta M > 0, M_{cur} > M_{max}^-$ (See Fig. A.1)	$\Delta\phi > 0, M_{cur} > M_{max}^-$ (See Fig. A.1)
4	6	$M_{cur} > M_{max}^+$	$M_{cur} > M_{max}^+$
	21	$M_{cur} < M_{max}^+$	$M_{cur} < M_{max}^+$
5	7	$M_{cur} < M_{max}^-$	$M_{cur} < M_{max}^-$
	20	$M_{cur} > M_{max}^-$	$M_{cur} > M_{max}^-$
6	8	$\Delta M > 0$	$\Delta\phi > 0$
	10	$\Delta M < 0$	$\Delta\phi < 0$

Note: $(\phi_{start}^i, M_{start}^i)$ and $(\phi_{end}^i, M_{end}^i)$ denote the start and end points of Branch "i"

Table A.6 Rules for Change of Branch (contd.)

7	9	$\Delta M < 0$	$\Delta \phi < 0$
	11	$\Delta M > 0$	$\Delta \phi > 0$
8	2	$M_{start}^2 < M_{end}^8 < M_{end}^2$, i.e., end point of Branch 8 lies on Branch 2	$\phi_{start}^2 < \phi_{end}^8 < \phi_{end}^2$, i.e., end point of Branch 8 lies on Branch 2
	4	Otherwise	Otherwise
9	3	$M_{start}^3 > M_{end}^9 > M_{end}^3$, i.e., end point of Branch 9 lies on Branch 3	$\phi_{start}^3 > \phi_{end}^9 > \phi_{end}^3$, i.e., end point of Branch 9 lies on Branch 3
	5	Otherwise	Otherwise
10	1	$\Delta M < 0$ and $M_{max}^- > M_y^-$, i.e., section has not yielded on the negative side	$\Delta \phi < 0$ and $M_{max}^- > M_y^-$, i.e., section has not yielded on the negative side
	12	$\Delta M < 0$ and $M_{max}^- < M_y^-$	$\Delta \phi < 0$ and $M_{max}^- < M_y^-$
	14	$\Delta M > 0$	$\Delta \phi > 0$
11	1	$\Delta M > 0$ and $M_{max}^+ < M_y^+$, i.e., section has not yielded on the positive side	$\Delta \phi > 0$ and $M_{max}^+ < M_y^+$, i.e., section has not yielded on the positive side
	13	$\Delta M > 0$ and $M_{max}^+ > M_y^+$	$\Delta \phi > 0$ and $M_{max}^+ > M_y^+$
	15	$\Delta M < 0$	$\Delta \phi < 0$
12	16	$\Delta M < 0$	$\Delta \phi < 0$
	20	$\Delta M > 0$	$\Delta \phi > 0$
13	17	$\Delta M > 0$	$\Delta \phi > 0$
	21	$\Delta M < 0$	$\Delta \phi < 0$

Note: $(\phi_{start}^i, M_{start}^i)$ and $(\phi_{end}^i, M_{end}^i)$ denote the start and end points of Branch "i"

Table A.6 Rules for Change of Branch (contd.)

14	2	$\Delta M > 0, M_{\max}^- < M_y^-$ (i.e., yielded on negative side), $M_{\max}^+ < M_y^+$ (i.e., not yielded on positive side) OR $\Delta M > 0, M_{\max}^- > M_y^-$ (i.e., not yielded on negative side), $M_{start}^2 < M_{end}^{14} < M_{end}^2$ (i.e., end point of Branch 14 lies on Branch 2)	$\Delta \phi > 0, M_{\max}^- < M_y^-$ (i.e., yielded on negative side), $M_{\max}^+ < M_y^+$ (i.e., not yielded on positive side) OR $\Delta \phi > 0, M_{\max}^- > M_y^-$ (i.e., not yielded on negative side), $\phi_{start}^2 < \phi_{end}^{14} < \phi_{end}^2$ (i.e., end point of Branch 14 lies on Branch 2)
	4	$\Delta M > 0, M_{\max}^- > M_y^-$ (i.e., not yielded on negative side), $M_{end}^{14} > M_{end}^2$ (i.e., end point of Branch 14 lies on Branch 4)	$\Delta \phi > 0, M_{\max}^- > M_y^-$ (i.e., not yielded on negative side), $\phi_{end}^{14} > \phi_{end}^2$ (i.e., end point of Branch 14 lies on Branch 4)
	13	$\Delta M > 0, M_{\max}^- < M_y^-$ (i.e., yielded on negative side), $M_{\max}^+ > M_y^+$ (i.e., yielded on positive side), $M_{start}^{13} < M_{end}^{14} < M_{end}^{13}$ (i.e., end point of Branch 14 lies on Branch 13)	$\Delta \phi > 0, M_{\max}^- < M_y^-$ (i.e., yielded on negative side), $M_{\max}^+ > M_y^+$ (i.e., yielded on positive side), $\phi_{start}^{13} < \phi_{end}^{14} < \phi_{end}^{13}$ (i.e., end point of Branch 14 lies on Branch 13)
	17	$\Delta M > 0, M_{\max}^- < M_y^-$ (i.e., yielded on negative side), $M_{\max}^+ > M_y^+$ (i.e., yielded on positive side), $M_{end}^{14} > M_{end}^{13}$ (i.e., end point of Branch 14 lies on Branch 17)	$\Delta \phi > 0, M_{\max}^- < M_y^-$ (i.e., yielded on negative side), $M_{\max}^+ > M_y^+$ (i.e., yielded on positive side), $\phi_{end}^{14} > \phi_{end}^{13}$ (i.e., end point of Branch 14 lies on Branch 17)
	24	$\Delta M < 0$	$\Delta \phi < 0$

Note: $(\phi_{start}^i, M_{start}^i)$ and $(\phi_{end}^i, M_{end}^i)$ denote the start and end points of Branch "i"

Table A.6 Rules for Change of Branch (contd.)

15	3	$\Delta M < 0, M_{\max}^+ > M_y^+$ (i.e., yielded on positive side), $M_{\max}^- > M_y^-$ (i.e., not yielded on negative side) OR $\Delta M < 0, M_{\max}^+ < M_y^+$ (i.e., not yielded on positive side), $M_{start}^3 > M_{end}^{15} > M_{end}^3$ (i.e., end point of Branch 15 lies on Branch 3)	$\Delta \phi < 0, M_{\max}^+ > M_y^+$ (i.e., yielded on positive side), $M_{\max}^- > M_y^-$ (i.e., not yielded on negative side) OR $\Delta \phi < 0, M_{\max}^+ < M_y^+$ (i.e., not yielded on positive side), $\phi_{start}^3 > \phi_{end}^{15} > \phi_{end}^3$ (i.e., end point of Branch 15 lies on Branch 3)
	5	$\Delta M < 0, M_{\max}^+ < M_y^+$ (i.e., not yielded on positive side), $M_{end}^{15} < M_{end}^3$ (i.e., end point of Branch 15 lies on Branch 5)	$\Delta \phi < 0, M_{\max}^+ < M_y^+$ (i.e., not yielded on positive side), $\phi_{end}^{15} < \phi_{end}^3$ (i.e., end point of Branch 15 lies on Branch 5)
	12	$\Delta M < 0, M_{\max}^+ > M_y^+$ (i.e., yielded on positive side), $M_{\max}^- < M_y^-$ (i.e., yielded on negative side), $M_{start}^{12} > M_{end}^{15} > M_{end}^{12}$ (i.e., end point of Branch 15 lies on Branch 12)	$\Delta \phi < 0, M_{\max}^+ > M_y^+$ (i.e., yielded on positive side), $M_{\max}^- < M_y^-$ (i.e., yielded on negative side), $\phi_{start}^{12} > \phi_{end}^{15} > \phi_{end}^{12}$ (i.e., end point of Branch 15 lies on Branch 12)
	16	$\Delta M < 0, M_{\max}^+ > M_y^+$ (i.e., yielded on positive side), $M_{\max}^- < M_y^-$ (i.e., yielded on negative side), $M_{end}^{15} < M_{end}^{12}$ (i.e., end point of Branch 15 lies on Branch 16)	$\Delta \phi < 0, M_{\max}^+ > M_y^+$ (i.e., yielded on positive side), $M_{\max}^- < M_y^-$ (i.e., yielded on negative side), $\phi_{end}^{15} < \phi_{end}^{12}$ (i.e., end point of Branch 15 lies on Branch 16)
	25	$\Delta M > 0$	$\Delta \phi > 0$

Note: $(\phi_{start}^i, M_{start}^i)$ and $(\phi_{end}^i, M_{end}^i)$ denote the start and end points of Branch "i"

Table A.6 Rules for Change of Branch (contd.)

22	3	$\Delta M < 0, M_{\max}^+ > M_y^+$ (I.e., yielded on positive side), $M_{\max}^- > M_y^-$ (i.e., not yielded on negative side) OR $\Delta M < 0, M_{\max}^+ < M_y^+$ (i.e., not yielded on positive side), $M_{start}^3 > M_{end}^{22} > M_{end}^3$ (i.e., end point of Branch 22 lies on Branch 3)	$\Delta \phi < 0, M_{\max}^+ > M_y^+$ (i.e., yielded on positive side), $M_{\max}^- > M_y^-$ (i.e., not yielded on negative side) OR $\Delta \phi < 0, M_{\max}^+ < M_y^+$ (i.e., not yielded on positive side), $\phi_{start}^3 > \phi_{end}^{22} > \phi_{end}^3$ (i.e., end point of Branch 22 lies on Branch 3)
	5	$\Delta M < 0, M_{\max}^+ < M_y^+$ (i.e., not yielded on positive side), $M_{end}^{22} < M_{end}^3$ (i.e., end point of Branch 22 lies on Branch 5)	$\Delta \phi < 0, M_{\max}^+ < M_y^+$ (i.e., not yielded on positive side), $\phi_{end}^{22} < \phi_{end}^3$ (i.e., end point of Branch 22 lies on Branch 5)
	12	$\Delta M < 0, M_{\max}^+ > M_y^+$ (i.e., yielded on positive side), $M_{\max}^- < M_y^-$ (i.e., yielded on negative side), $M_{start}^{12} > M_{end}^{22} > M_{end}^{12}$ (i.e., end point of Branch 22 lies on Branch 12)	$\Delta \phi < 0, M_{\max}^+ > M_y^+$ (i.e., yielded on positive side), $M_{\max}^- < M_y^-$ (i.e., yielded on negative side), $\phi_{start}^{12} > \phi_{end}^{22} > \phi_{end}^{12}$ (i.e., end point of Branch 22 lies on Branch 12)
	16	$\Delta M < 0, M_{\max}^+ > M_y^+$ (i.e., yielded on positive side), $M_{\max}^- < M_y^-$ (i.e., yielded on negative side), $M_{end}^{22} < M_{end}^{12}$ (i.e., end point of Branch 22 lies on Branch 16)	$\Delta \phi < 0, M_{\max}^+ > M_y^+$ (i.e., yielded on positive side), $M_{\max}^- < M_y^-$ (i.e., yielded on negative side), $\phi_{end}^{22} < \phi_{end}^{12}$ (i.e., end point of Branch 22 lies on Branch 16)
	20	$\Delta M > 0$	$\Delta \phi > 0$

Note: $(\phi_{start}^i, M_{start}^i)$ and $(\phi_{end}^i, M_{end}^i)$ denote the start and end points of Branch "i"

Table A.6 Rules for Change of Branch (contd.)

23	2	$\Delta M > 0, M_{\max}^- < M_y^-$ (i.e., yielded on negative side), $M_{\max}^+ < M_y^+$ (i.e., not yielded on positive side) OR $\Delta M > 0, M_{\max}^- > M_y^-$ (i.e., not yielded on negative side), $M_{start}^2 < M_{end}^{23} < M_{end}^2$ (i.e., end point of Branch 23 lies on Branch 2)	$\Delta \phi > 0, M_{\max}^- < M_y^-$ (i.e., yielded on negative side), $M_{\max}^+ < M_y^+$ (i.e., not yielded on positive side) OR $\Delta \phi > 0, M_{\max}^- > M_y^-$ (i.e., not yielded on negative side), $\phi_{start}^2 < \phi_{end}^{23} < \phi_{end}^2$ (i.e., end point of Branch 23 lies on Branch 2)
	4	$\Delta M > 0, M_{\max}^- > M_y^-$ (i.e., not yielded on negative side), $M_{end}^{23} > M_{end}^2$ (i.e., end point of Branch 23 lies on Branch 4)	$\Delta \phi > 0, M_{\max}^- > M_y^-$ (i.e., not yielded on negative side), $\phi_{end}^{23} > \phi_{end}^2$ (i.e., end point of Branch 23 lies on Branch 4)
	13	$\Delta M > 0, M_{\max}^- < M_y^-$ (i.e., yielded on negative side), $M_{\max}^+ > M_y^+$ (i.e., yielded on positive side), $M_{start}^{13} < M_{end}^{23} < M_{end}^{13}$ (i.e., end point of Branch 23 lies on Branch 13)	$\Delta \phi > 0, M_{\max}^- < M_y^-$ (i.e., yielded on negative side), $M_{\max}^+ > M_y^+$ (i.e., yielded on positive side), $\phi_{start}^{13} < \phi_{end}^{23} < \phi_{end}^{13}$ (i.e., end point of Branch 23 lies on Branch 13)
	17	$\Delta M > 0, M_{\max}^- < M_y^-$ (i.e., yielded on negative side), $M_{\max}^+ > M_y^+$ (i.e., yielded on positive side), $M_{end}^{23} > M_{end}^{13}$ (i.e., end point of Branch 23 lies on Branch 17)	$\Delta \phi > 0, M_{\max}^- < M_y^-$ (i.e., yielded on negative side), $M_{\max}^+ > M_y^+$ (i.e., yielded on positive side), $\phi_{end}^{23} > \phi_{end}^{13}$ (i.e., end point of Branch 23 lies on Branch 17)
	21	$\Delta M < 0$	$\Delta \phi < 0$

Note: $(\phi_{start}^i, M_{start}^i)$ and $(\phi_{end}^i, M_{end}^i)$ denote the start and end points of Branch "i"

Table A.6 Rules for Change of Branch (contd.)

16	4	$\Delta M < 0$	$\Delta \phi < 0$
	20	$\Delta M > 0$	$\Delta \phi > 0$
17	5	$\Delta M > 0$	$\Delta \phi > 0$
	21	$\Delta M < 0$	$\Delta \phi < 0$
20	11	$\Delta M > 0$	$\Delta \phi > 0$
	22	$\Delta M < 0$	$\Delta \phi < 0$
21	10	$\Delta M < 0$	$\Delta \phi < 0$
	23	$\Delta M > 0$	$\Delta \phi > 0$
24	10	$\Delta M < 0$	$\Delta \phi < 0$
	14	$\Delta M > 0$	$\Delta \phi > 0$
25	11	$\Delta M > 0$	$\Delta \phi > 0$
	15	$\Delta M < 0$	$\Delta \phi < 0$

Note: $(\phi_{start}^i, M_{start}^i)$ and $(\phi_{end}^i, M_{end}^i)$ denote the start and end points of Branch “*i*”

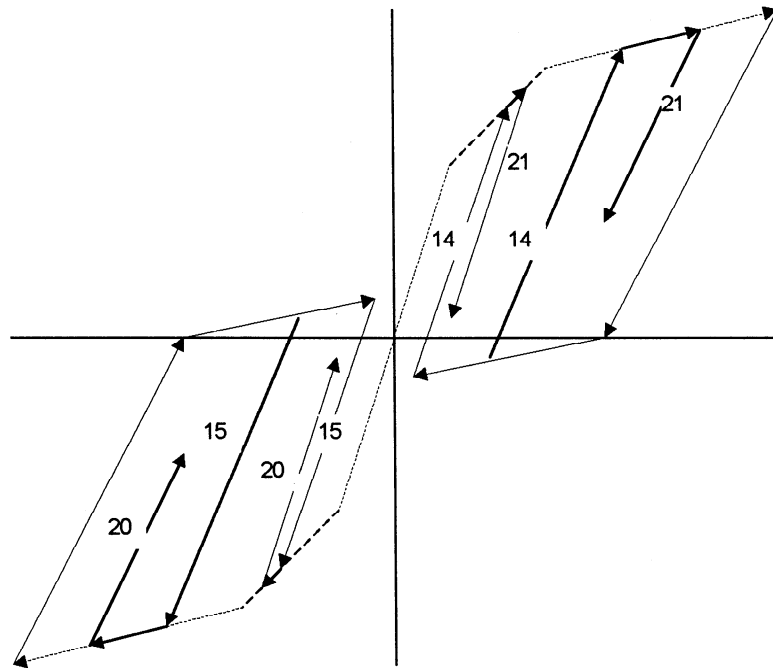



Fig. A.1 Explanation for Rules which change Branches from 2 to 21 and 3 to 20



MULTIDISCIPLINARY CENTER FOR EARTHQUAKE ENGINEERING RESEARCH

A National Center of Excellence in Advanced Technology Applications

University at Buffalo, State University of New York
Red Jacket Quadrangle ■ Buffalo, New York 14261-0025
Phone: 716/645-3391 ■ Fax: 716/645-3399
E-mail: mceer@acsu.buffalo.edu ■ WWW Site: <http://mceer.buffalo.edu>



University at Buffalo *The State University of New York*

ISSN 1520-295X